


ORIGINAL ARTICLE OPEN ACCESS

Integrating Load-Cell Lysimetry and Machine Learning for Prediction of Daily Plant Transpiration

Shani Friedman  | Nir Averbuch | Tifferet Nevo | Menachem Moshelion

The Robert H. Smith Institute of Plant Sciences and Genetics in Agriculture, The Robert H. Smith Faculty of Agriculture, Food and Environment, The Hebrew University of Jerusalem, Rehovot, Israel

Correspondence: Menachem Moshelion (menachem.moshelion@mail.huji.ac.il)

Received: 5 December 2024 | **Revised:** 17 September 2025 | **Accepted:** 19 September 2025

Funding: This study was partly supported by the Shoenberg Research Center for Agricultural Science (Grant No. 3175006230), the Israel Science Foundation (Grant No. 1043/20) and the Israeli Committee for Budgeting, which support research on sustainable agriculture and food security at the Israeli Center for Digital Agriculture. This project was also funded by the Planning and Budgeting Committee of the Council for Higher Education in Israel (VATAT) as part of the programme 'Israeli Center for Digital Agriculture'.

Keywords: artificial intelligence | feature importance | gravimetric lysimeters | irrigation management | machine learning (ML) | Penman–Monteith | precision agriculture | transpiration-prediction

ABSTRACT

We conducted research to predict daily transpiration in crops by utilising a combination of machine learning (ML) models combined with extensive transpiration data from gravimetric load cells and ambient sensors. Our aim was to improve the accuracy of transpiration estimates. Data were collected from hundreds of plant specimens growing in two semi-controlled greenhouses over 7 years, automatically measuring key physiological traits (serving as our ground truth data) and meteorological variables with high temporal resolution and accuracy. We trained Decision Tree, Random Forest, XGBoost and Neural Network models on this data set to predict daily transpiration. The Random Forest and XGBoost models demonstrated high accuracy in predicting the whole plant transpiration, with R^2 values of 0.89 on the test set (cross-validation) and $R^2 = 0.82$ on holdout experiments. Ambient temperature was identified as the most influential environmental factor affecting transpiration. Our results emphasise the potential of ML for precise water management in agriculture, and simplify some of the complex and dynamic environmental forces that shape transpiration.

1 | Introduction

Transpiration, the process of water evaporation from plants, has been a subject of scientific studies for centuries. It primarily occurs through leaves, facilitating a continuous transport of water and essential nutrients from the roots. One remarkable aspect of transpiration is how plants regulate it in response to their surroundings through dynamic control mechanisms. This process is intricately linked to the behaviour of stomata, small pores found on the leaf surface. Stomata can adjust their aperture to manage the rate of transpiration (Lange et al. 1971).

This adaptive response to the environment appears to have evolved as one of the protective mechanisms against excessive dehydration and physiological damage (Iqbal et al. 2020).

The dynamic ability of plants to regulate their transpiration rates plays a vital role in facilitating the exchange of carbon dioxide and water, thereby improving water use efficiency and optimising growth. Various factors, both biological, such as plant size (Geller and Smith 1982) and environmental such as solar Radiation (Pieruschka et al. 2010), temperature (Ben-Asher et al. 2008), humidity (Rawson et al. 1977), soil water supply (Madhu and

Shani Friedman and Nir Averbuch contributed equally to this article.

This is an open access article under the terms of the [Creative Commons Attribution-NonCommercial-NoDerivs](https://creativecommons.org/licenses/by-nc-nd/4.0/) License, which permits use and distribution in any medium, provided the original work is properly cited, the use is non-commercial and no modifications or adaptations are made.

© 2025 The Author(s). *Plant, Cell & Environment* published by John Wiley & Sons Ltd.

Hatfield 2014), carbon dioxide levels (Imai and Murata 1976; Madhu and Hatfield 2014) and wind speed (Dixon and Grace 1984), can impact the transpiration rates of different plants. The understanding of these influential factors holds paramount significance in the fields of agriculture and ecophysiological sciences.

Understanding and quantifying the factors which affect transpiration and plant-water relations has a key role in optimising water management strategies in agricultural and greenhouse settings. Therefore, various modelling approaches have been employed to simulate and evaluate transpiration rates in plants. One common approach is the use of mechanistic models, which are based on physiological principles and the understanding of plant structure and function. For example, the semi-empirical Ball–Berry model integrates stomatal conductance and environmental variables to estimate transpiration rates (Ball et al. 1987). However, it is important to note that the Ball–Berry model simplifies the complex process, assuming a linear relationship between stomatal conductance and photosynthesis, which can significantly influence stomatal behaviour and transpiration rates.

In contrast, process-based models like the Penman–Monteith equation take a more comprehensive approach. Process-based models represent a modelling approach that simulates natural processes by representing the underlying mechanisms. Penman–Monteith equation combines energy balance and aerodynamic principles to predict evapotranspiration (ET) (Monteith 1965; Penman 1948). The FAO56 Penman–Monteith is commonly used in the agriculture community to estimate ET (Landeras et al. 2008). However, previous studies have found that daily FAO56 Penman–Monteith exhibited up to 22% discrepancy in accuracy compared to the actual whole-plant transpiration measured using lysimeters (Averbuch and Moshelion 2024; Kiraga et al. 2023; López-Urrea et al. 2006). These discrepancies underscore the ongoing need for improvement and refinement in modelling techniques to better understand and predict transpiration in different conditions and environments.

Recent studies and reviews consistently show that machine learning models such as artificial neural networks (ANN) and support vector regression outperform conventional empirical models in estimating ET across diverse climates. These have shown promising results in estimating transpiration based on environmental inputs and plant characteristics (Amani and Shafizadeh-Moghadam 2023; Balasubramanian and Thirugnanam 2023; Meneses et al. 2020; Ferreira et al. 2019; Xing et al. 2016, 2022). However, many of these studies rely on broad or indirect data labels (e.g., remote sensing, estimated transpiration, or synthetic data) that do not fully capture the detailed plant–environment interactions critical for accurate physiological modelling. To extend our understanding of how machine learning has been applied in this field, we conducted a systematic search of the Scopus database for relevant studies (for more details, see Methods S1). Among these, 33.9% (184 articles) employed indirect estimation methods, primarily remote sensing (150 articles) and eddy covariance (34 articles), while empirical models like FAO-56 Penman–Monteith appeared in 26.0% (141 articles). However, only 4.8% (26 articles) included keywords related to direct physiological measurements, such as sap flow sensors, load cells, lysimeters,

porometry, or gas exchange systems—highlighting a clear gap in capturing direct plant–environment interactions.

Among the relatively few studies that applied direct physiological measurements, most relied on low-throughput, leaf-level methods. For example, stomatal conductance has been assessed using porometers or gas-exchange systems to train ML models, with recent work showing that ML can outperform traditional approaches in predicting stomatal behaviour (Gaur and Drewry 2024; Saunders et al. 2021). Yet because these methods are labour-intensive and restricted to individual leaves, they often depend on compiled public or synthetic gas-exchange data sets (Anderegg et al. 2018; Lin et al. 2015).

Accurately modelling whole-plant transpiration remains a major challenge because it is a highly dynamic process regulated by thousands of signalling and transport processes within the plant and influenced by multiple, interdependent environmental variables. To capture this complexity, ML models must be trained on reliable, high-resolution physiological ground truth data that reflect actual plant behaviour—not estimated or proxy data streams. Sap-flow sensors have been employed as labels for ML models in crops such as tomato and maize, where Random Forest and deep learning approaches achieved high predictive accuracy (Amir et al. 2021; Fan et al. 2021). However, these sensors may damage tissue, alter water transport and lose accuracy over time (Kumar et al. 2022). In contrast, load-cells lysimeters are widely regarded as the gold standard for measuring whole-plant transpiration, as they enable direct quantification of ET or transpiration flux (Halperin et al. 2017). ML models trained on data derived from lysimeters can serve as reliable benchmarks (‘ground truth’) for validating or calibrating alternative indirect estimation methods (Amani and Shafizadeh-Moghadam 2023; Anapalli et al. 2016; X. Liu et al. 2017).

Despite their benefits, most lysimeter-based studies have relied on either drainage or manual lysimeters, typically in small numbers because of their high cost and labour-intensive maintenance (Z. Chen et al. 2020; Kiraga et al. 2023). Examples include two weighing units in alfalfa (Kiraga et al. 2023) and maize (Z. Chen et al. 2020), four drainage units in garlic (Abyaneh et al. 2010) and six weighing units for tomato (Li et al. 2020). Even larger installations, such as the 64 drainage lysimeters used by Sperling et al. (2023) in almond orchards, were constrained by low temporal resolution, with drainage recorded only every 14 days. Our approach, by contrast, leverages a high-throughput load-cells lysimeter platform, with a high signal-to-noise ratio, enabling large-scale, directly labelled data sets suitable for robust model training.

In this study, we focused on whole plant daily measurements of transpiration for Mediterranean summer and winter crops, tomato and cereals (Wheat and Barley), respectively. Over the past 7 years, we have collected a precise data set of direct physiological traits from hundreds of plant specimens, along with corresponding environmental data. Leveraging this unique data set, we employed machine learning models to predict the daily transpiration of well-irrigated plants. Our data are distinguished by their high scale and the use of ground truth annotated physiological measurements (e.g., whole plant

transpiration g/day). These are obtained from an extensive array of load cells lysimeters and atmospheric conditions.

The objectives of this study were to: (1) evaluate the effectiveness of conventional tree-based machine learning models, including Random Forest, an XGBoost model and a neural network model, in predicting daily transpiration for tomato and cereal crops; and (2) determine the hierarchical significance of diverse ambient factors, thereby pinpointing the critical environmental factors that exert influence on transpiration.

2 | Materials and Methods

2.1 | Research Overview

In this study, we aimed to understand the determinants of daily transpiration in plants using a structured machine learning research workflow. Data collection took place within semi-commercial greenhouses using a functional phenotyping platform composed of load-cells lysimeters. This platform provided essential information on several plant physiological traits (transpiration, plant biomass, growth rate etc.) and ambient conditions. After essential data pre-processing steps, including outlier removal and transformation to daily values, we had 6115 observations (81% of the original daily data), split into training and testing sets. Machine learning models, including tree-based models and neural networks, were trained to predict daily transpiration using the features: plant biomass, temperature, humidity, Daily Light Integral (DLI), vapour pressure deficit (VPD), plant type and soil type. Model evaluation encompassed various metrics such as R^2 and root mean square error (RMSE). Model interpretation was accomplished through the analysis of feature importance using techniques like Permutation and Shapley Additive Explanations (SHAP; see Section 2.9). These methods hold major contribution to understanding the different features of the models' predictions and their impact on daily transpiration. This workflow allowed us to gain valuable insights into the determinants of daily transpiration in plants.

2.2 | Experimental Site

Data were collected from two semi-controlled greenhouses located at the I-CORE centre for Functional Phenotyping of the Faculty of Agriculture, Food and Environment in Rehovot, Israel (<http://departments.agri.huji.ac.il/plantscience/icore.php>). The 'main greenhouse' (Figure 1) is a polycarbonate-covered structure at coordinates 31°54'15.0"N, 34°48'03.6"E, measuring 18 m in length and 16 m in width, with a gutter height of 4.5 m and a maximum ridge height of 6 m (dual-gable structure). The estimated internal volume, based on an average height of 5.25 m, is approximately 1417.5 m³. The 'secondary greenhouse' (Figure 1B), also polycarbonate covered, located at 31°54'22.5" N, 34°48'10.6" E, spans 6 × 17 m² and reaches a height of 3 m.

Both facilities feature natural daylight conditions and are equipped with a cooling pad along the northern wall to maintain temperatures below 35°C. Ventilation is achieved by using a positive pressure cooling system, where outside air is pushed into the greenhouse through a wet pad by four fans, each with

capacity of 18 000 m³/h, totalling flow rate of 72 000 m³/h (This setup enables an air exchange rate of approximately 51 air changes per hour, for the main greenhouse). The fans are automatically activated about 30 min before sunrise and turned off about 30 min after sunset to ensure consistent airflow during the photoperiod. This high ventilation rate is designed to maintain CO₂ concentrations similar to those in the ambient outdoor air, facilitating natural plant responses. To complement these efforts and further simulate natural external conditions, wind speed and direction are precisely monitored using an ATMOS 22 ultrasonic anemometer, centrally located in the main greenhouse. This sensor records an average wind speed of 0.324 m/s. For both greenhouses, the experimental conditions varied, with natural DLI values ranging from 2 to 34 mol/(m²·day) and mean daily temperatures fluctuating between 10°C and 33°C (Table S1A).

2.3 | General Experiment Setup and Data Collection

The data were collected from June 2018 to March 2024. Using the functional phenotyping platform—PlantArray (PlantDitech, Israel; Figure 1C) as described by Dalal et al. 2020; Halperin et al. 2017. Briefly, an array of load cell lysimeters was utilised (Figure 1), to continuous plant weight measurement and the derivation of both transpiration-induced water loss and daily plant mass accumulation. To ensure that water loss reflects plant transpiration only, the surface of the soil in each pot was sealed to prevent soil evaporation (Figure 1D). All data were automatically collected and uploaded to the cloud-base SPAC analytics system (PlantDitech, Israel).

Meteorological data, consisting of four essential variables—temperature, VPD, light and relative humidity (RH), were collected using a weather station (Watchdog 2000 series; Spectrum Technologies, Illinois, USA) connected to the PlantArray system. Within each greenhouse, the atmospheric sensors were positioned at the centre of the greenhouse, approximately 1 m above the height of the pot surface (Figure 1C).

The lysimeter-based phenotyping system employed several strategies to enhance the signal-to-noise ratio, thereby reducing potential artefacts in the noisy greenhouse environment. These strategies include the use of high-accuracy load cell transducers, achieving a precision of ±0.167 g per kg loaded on each cell. These transducers are also temperature-compensated to effectively minimise signal drift caused by ambient temperature fluctuations. Furthermore, each load cell is connected via a short cable (45 cm) to its individual analogue-to-digital (A/D) controller, significantly reducing analogue electrical interference and noise (typically associated with long cables connected to a single data logger). To prevent overheating due to direct solar radiation, thermal insulation and sealed covers are applied separately to each load cell. In addition, vibration-induced noise is mitigated by placing compressed foam cushions and mass under each load cell. Measures to counteract the 'pot effect' (Gosa et al. 2019), such as double-pot arrangements isolating the soil and roots from direct solar radiation-induced heat, to ensure the reliability and consistency of the physiological data collected during the experiment (Figure 1E).

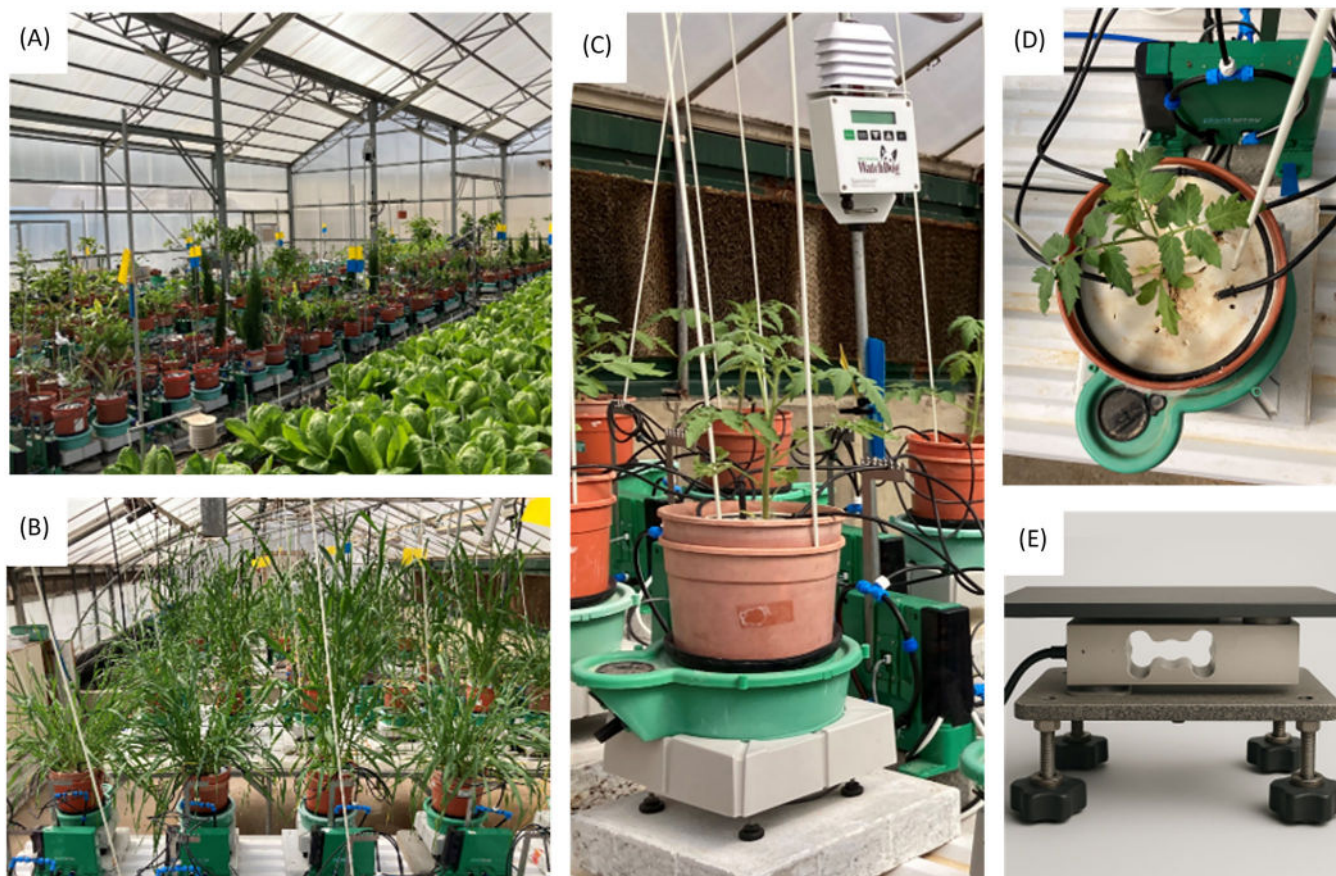


FIGURE 1 | Configuration of the load cell lysimeter system and greenhouse. (A) Main greenhouse containing various crops monitored using the PlantArray phenotyping platform. (B) Secondary greenhouse with wheat plants monitored using the same system. (C) Image of a single PlantArray unit, showing the load-cell lysimeter, double-pot setup, 'personalise' controller collecting data and controlling each pot irrigation, and the central weather station used for continuous environmental monitoring. (D) Top view of a pot showing the sealed soil surface cover, designed to isolate plant transpiration from soil evaporation. (E) Photorealistic illustration of a single lysimeter unit. It includes a temperature-compensated load cell that converts mechanical force into an electrical signal, directly connected to the controller. The cell is mounted between two steel platforms to ensure stable weight measurement. As shown in C, the lysimeter is typically covered with a polystyrene block and a thermal-isolated lid. [Color figure can be viewed at [wileyonlinelibrary.com](https://onlinelibrary.wiley.com)]

2.3.1 | Plant Material and Growing Media

The plants in the greenhouse were grown in pots (4 L) filled with sand (Silica sand grade 20–30, particle size 0.595–0.841 mm; Negev Industrial Minerals Ltd., Yeruham, Israel) or soil (Bentel 11 garden mix, composed of (w/w) 55% peat, 20% tuff and 25% puffed coconut coir fibre; Tuff-Substrates, Alon Tavor, Israel).

Tomato, wheat and barley (cereals), were employed in this experiment. The tomato (*Solanum lycopersicum*) variety incorporated in the study was mainly the M82 cultivar. The cereals included *T. turgidum subsp. durum* 'Svevo' and *T. aestivum cv. Gadish*, among others. Focusing on these commonly cultivated crops, ensuring multiple repetitions and capturing the diversity of both winter and summer representations.

2.3.2 | Irrigation and Water Balance Measurements

All pots were irrigated through repeated irrigation and drainage cycles every night, reliably restoring the soil to field capacity (hereafter referred to as 'well-irrigated'). This approach not only

maintained optimal soil moisture levels but also facilitated leaching to prevent salt accumulation. Daily pre-dawn pot mass was measured after full drainage. Plant mass was calculated at this point. The difference in pot mass between consecutive days reflects the plant's biomass gain. The lack of additional irrigation throughout the daylight hours ensured a monotonic pot-mass decrease between subsequent irrigation events. Transpiration was calculated based on the mass loss during the day. For full details on calculations and system, see Dalal et al. (2020) and Halperin et al. (2017).

In this study, we focused exclusively on non-stressed plants by ensuring that soil water content consistently remained above the transpiration-limiting threshold (Halperin et al. 2017). This was achieved by selecting data exclusively from control (non-drought) treatments, while deliberately excluding any data from plants that surpassed their pot's capacity, thereby ensuring non-pot effect of draught conditions. Therefore, we checked the data manually, removing entries where plants exhibited 'pot limitation', a scenario where a plant's transpiration plateaus due to reaching the pot's maximum available water capacity. While the calculated total water-holding capacity is approximately 860 g in sand and 1700 g in

potting media (Dalal et al. 2020), the actual available water for plants is lower: around 600 g/day in sand and 1200 g/day in soil, influenced by root structure and soil properties.

2.4 | Data Pre-Processing

The data were initially collected at 3-min intervals. For this study, it was further processed to generate daily values, covering the period from first light to last light (Table 1). Using daily values reduces the total data volume to balance capturing environmental variability while keeping data processing manageable. Moreover, this simplifies data interpretation, making it practical for applications such as irrigation decisions, much like other common methods, including the FAO56 Penman–Monteith model for irrigation management.

The type of potting media (sand or soil) and the specific plant species (tomato or cereal) were recorded. Light data in terms of Photosynthetically Active Radiation (PAR) was measured at 3-min intervals. The DLI was calculated using the formula:

$$DLI \left(\frac{\text{mol}}{\text{m}^2 \times \text{day}} \right) = \frac{\sum \text{PARlight} \left(\frac{\mu\text{mol}}{\text{m}^2\text{s}} \right)}{n} \times 86\,400 \left(\frac{\text{sec}}{\text{day}} \right) \times \frac{1 \text{ mol}}{1\,000\,000 \mu\text{mol}} \quad (1)$$

TABLE 1 | Data set description and the main preprocessing methods.

Category	Variable	Units	Description
ID	Timestamp		Date
	Icore greenhouse		The greenhouse from which the data were collected, encoded as Main = 1 and secondary = 0.
	ExpId		Experiment number: Each independent experiment contained 1–10 plants (repetitions) that the data were collected simultaneously from. A total of 48 independent experiments were used.
	PlantId		The plant-specific ID number, each plant was measured continuously for about 3–4 weeks. On average 23 daily observations per-plant. A total of 269 plants were used.
Meteorology	Temperture	°C	The average temperature at daytime (from the first to last light).
	RH	%	The average Relative Humidity at daytime (from the first to last light).
	VPD	kPa	The average Vapour Pressure Deficit (VPD) at daytime (from the first to last light).
	DLI	mol/m ² × day	Daily Light Integral (DLI) was calculated using Formula 1.
Others	Potting media		‘Encoded soil’—dummy variables, 0 = silica sand, 1 = soil (4508 and 1607 observation respectively).
	Plant types		‘Encoded plant’—dummy variable, 0 = tomato, 1 = cereal (3975 and 2140 observation, respectively)
Plant weight	Plant biomass	g	The net weight of the plant as calculated at 4AM, after soil field capacity (for details see Halperin et al. 2017).
	Transpiration	g	Daily water evaporating through the plant (for details see Halperin et al. 2017). This variable was used as output for the models.

where n is the number of samples in a full day (480 if sampled every 3 min). $\sum \text{PARlight} \left(\frac{\mu\text{mol}}{\text{m}^2\text{s}} \right)$ is the sum of PAR light measurements throughout the day.

This calculation provided insights into the cumulative light exposure experienced by the plants over the course of a day.

Our data set initially included 7547 observations, where each observation represented a single plant measured on a given day. An example of an individual plant is illustrated in Figure 2. After a comprehensive data cleaning process, we concluded with a total of 6115 observations. This reduction was due to the removal of observations with missing values, extreme outliers and those exhibiting irregular behaviours such as weight loss, water shortage, or illnesses. The final variables and some preprocessing methods, such as daily aggregation of values and encoding, are detailed in Table 1.

2.5 | Tuning, Training and Testing Data Sets

After preprocessing, the data set comprised 6115 daily observations. Figure 2 illustrates a sample plant with 24 observations. Figure 3 presents the full data set from the main greenhouse, including meteorological and aggregated physiological data. The feature variables included Temperature, RH, VPD, DLI,

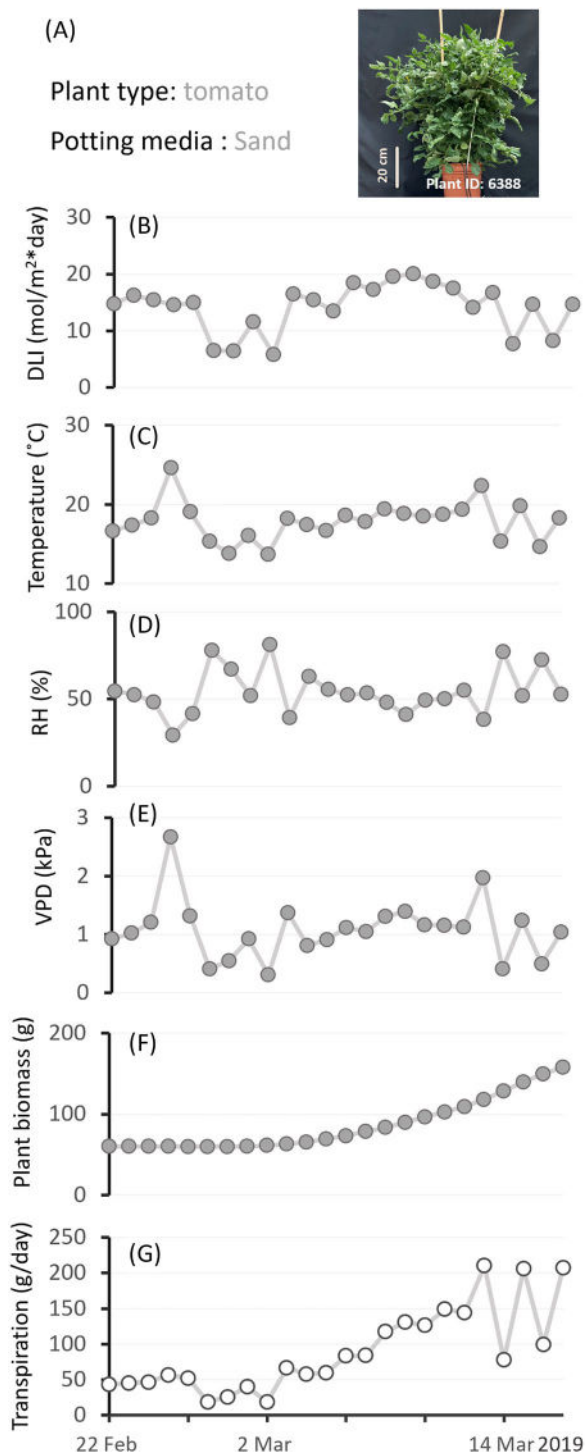


FIGURE 2 | Representative meteorological and physiological data derived from the I-core greenhouse PlantArray system. This figure presents data from a single plant as an example. (A) Plant identity information: plant type, potting media, ID number and plant picture at the end of the experiment. Daily average of (B) light integral, (C) temperature, (D) relative humidity and (E) vapour pressure deficit over a period of 22 days. (F) Plant biomass—plant net weight (G), whole-plant daily transpiration, highlighting the sensitivity of the transpiration to the methodological changes. Filled grey circles indicate input (X) variables, and open circles indicate output (Y) variables used for model training and prediction. [Color figure can be viewed at [wileyonlinelibrary.com](https://onlinelibrary.wiley.com)]

plant biomass, plant type and soil type, with the target variable being daily transpiration (Figure 2, Table 1).

2.5.1 | Validation Data Set (Holdout)

To assess the model's generalisability, a holdout data set comprising 805 observations from four randomly selected experiments was established, a random seed function was set to ensure repeatability. This subset includes 400 observations related to tomato plants and 405 observations concerning cereal plants (for more information, see Table S1b and Figure S1b). This holdout data set aims to reflect the model's performance and effectiveness on unseen data.

2.5.2 | Training Data Set

Ninety percent (4779 observations) of the remaining data was randomly selected to tune the hyperparameters, as detailed in Section 2.7. This initial subset helped determine the optimal hyperparameters, allowing us to assess the effectiveness of the tuning process. After selecting the best hyperparameters, the models were then trained on the full data set, excluding the holdout set (in total 5310 observations). This approach ensures that the final model training incorporates the broadest data spectrum available while retaining an independent holdout set to evaluate the model (see Section 2.9).

2.6 | Machine Learning Models for Estimating Daily Transpiration

2.6.1 | Decision Tree

Decision trees are a simple, yet powerful machine learning model used for classification and regression tasks. They recursively split the data into subsets based on the features to create a tree-like structure. At each node, the decision tree selects the feature and split point that minimises impurity, aiming to create more homogenous subsets. The final predictions are made based on average value (for regression) of the samples in the leaf nodes. Decision trees are interpretable and can capture complex relationships in the data, but they may suffer from overfitting and lack generalisation ability. The induction of decision trees is one of the oldest and most popular techniques for learning discriminatory models, which has been developed independently in the statistical (Breiman et al. 1984; Mingers 1989) and machine learning (Quinlan 1993) communities (Fürnkranz 2011).

2.6.2 | Random Forest

Random Forest is an ensemble learning technique based on decision trees. It builds multiple decision trees, each trained on a random subset of the data and a random subset of the features. The final prediction is obtained by averaging (for regression) the predictions of individual trees. Random Forest overcomes the overfitting issue of decision trees and improves the model's performance and robustness. It can handle high-dimensional

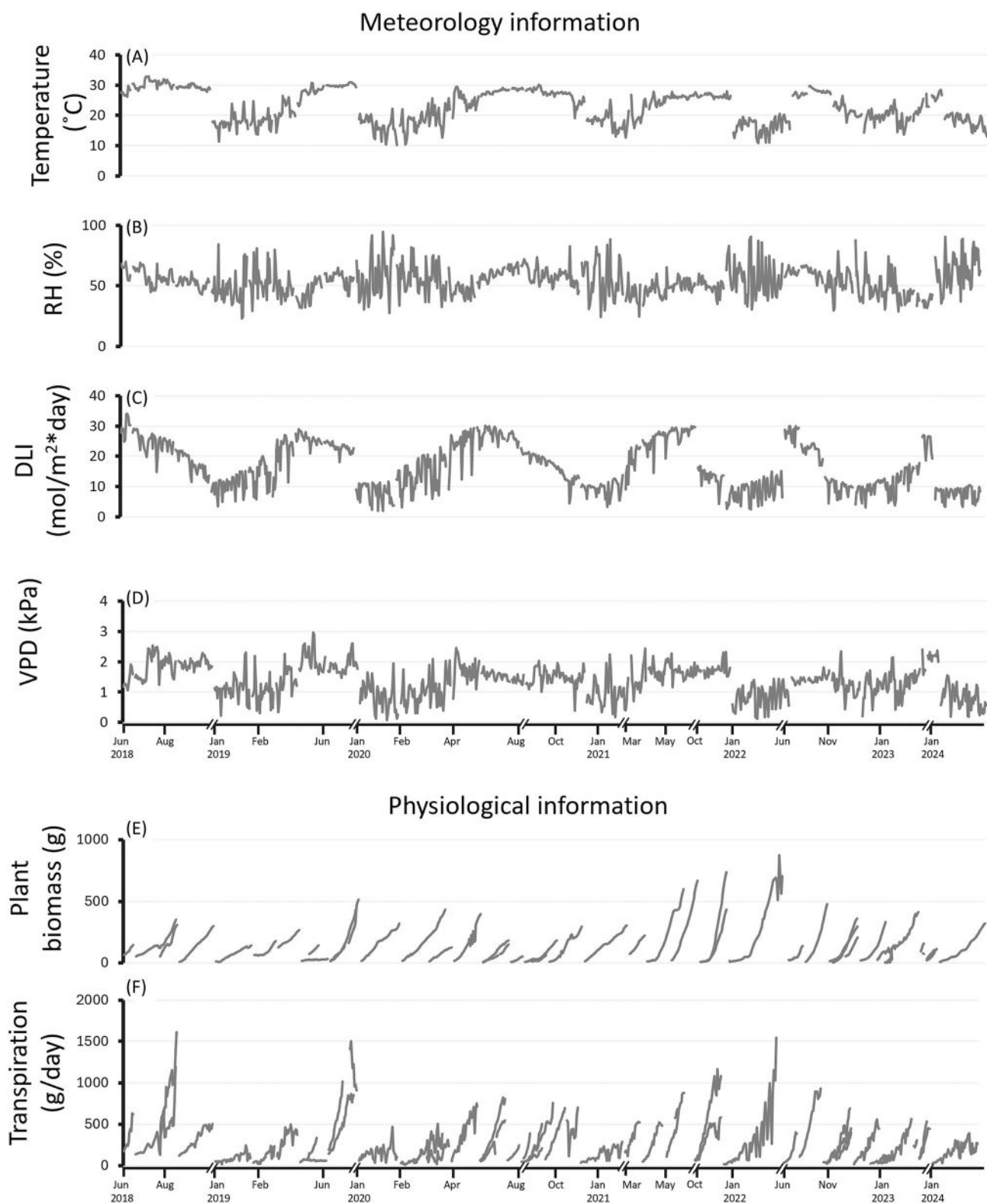


FIGURE 3 | Summary of meteorological and physiological data collected in the main I-CORE greenhouse over the entire study period. This figure presents the full data set collected from the PlantArray lysimeter system across multiple experiments conducted in the main greenhouse. Panels (A–D) show daily average meteorological conditions: (A) daily light integral (DLI), (B) temperature, (C) relative humidity (RH) and (D) vapour pressure deficit (VPD), recorded continuously throughout the experiments timeline. Panels (E, F) present physiological responses averaged across all plants measured in each experiment. (E) Average plant biomass, illustrating the typical pattern of plant development, where plants begin small and progressively accumulate biomass over time. (F) Average daily transpiration per plant, reflecting physiological responses to both environmental conditions and developmental stage. Gaps along the x-axis correspond to time periods when no relevant experiments were conducted or when the greenhouse was inactive. Note that different experiments may overlap in time.

data sets and capture interactions between features, making it a popular choice for various applications.

The random forest or decision tree forest is an algorithm created in 1995 by Ho (1995), then formally proposed by scientists in 2001 (Breiman 2001; Cutler and Zhao 2001).

2.6.3 | XGBoost Model

eXtreme Gradient Boosting (XGBoost) is a method, initially proposed by T. Chen and Guestrin (2016), which generally generates high accuracy and fast processing time while being computationally less costly and less complex. The XGBoost model is a scalable machine learning system for tree boosting. The XGBoost model integrates several 'weak' learners for developing a 'strong' learner through additive learning. Parallel computation is automatically implemented during training to enhance computational efficiency (Fan et al. 2021).

2.6.4 | ANN

Neural networks are a class of deep learning models inspired by the structure and function of the human brain (Haykin 2009; Rosenblatt 1958). They consist of interconnected nodes (neurons) organised into layers. Each node applies an activation function to the weighted sum of its inputs to produce an output (Fukushima 1969). As many ML models, Neural networks can learn complex and nonlinear relationships in the data through the process of forward and backward propagation during training (Leibniz 1920).

2.7 | Hyperparameters Tuning

Hyperparameter tuning is the process of discovering the optimal configuration for the hyperparameters of a machine learning model to achieve the best performance. Hyperparameters are external configuration settings established before the training process and are not learned from the data. Examples included learning rates, regularisation strengths and the number of trees in a random forest.

This process of hyperparameter tuning was carried out through cross-validation grid search on the training data. Grid search cross-validation is a method employed to systematically explore a vast array of combinations of hyperparameter values. By leveraging five-fold cross-validation, the data set was divided into five subsets, allowing for multiple rounds of training and validation. This approach aimed to find the optimal set of hyperparameter values and ensure the model's robustness by evaluating its performance across different subsets of the training data. The optimal hyperparameter values and the options we tested are summarised in Table 2.

2.8 | Modelling Process

We implemented our models using a robust set of Python libraries tailored for statistical computing, data manipulation and machine

learning. Specifically, we used: Scipy (Virtanen et al. 2020), for conducting statistical tests, Numpy (Harris et al. 2020), for high-performance numerical operations, Pandas (McKinney 2010; The pandas development team 2020), for data handling and manipulation, Sklearn (Pedregosa et al. 2011) for machine learning algorithms and model evaluation tools, Keras (Chollet 2015) and TensorFlow (Abadi et al. 2016) for building and training neural network models.

2.9 | Cross-Validation and Performance Evaluation

Cross-validation was conducted on the data set to validate model stability and reliability. We used 10-fold cross-validation, allowing each subset of data to be used as both training and testing sets iteratively, ensuring comprehensive performance assessment. This method not only helps in assessing the performance across different slices of data but also in comparing the effectiveness of different models under varying conditions (Table 3).

The final model evaluation was performed on the holdout set, using metrics such as RMSE, mean absolute error (MAE) and the R^2 statistic to compare the predictions and actual measurements (Table 4). These metrics provided a detailed measure of model accuracy, prediction error and the proportion of variance explained by the model.

2.10 | Model Validation Using External Greenhouse and Growth Room Data

To further evaluate the generalisability of our machine learning models, we tested their performance on two external data sets collected independently from the training and validation data. The first data set was obtained from a greenhouse facility located in Tel Aviv University, operated entirely by a different research group, using separate personnel, experimental planning and management protocols. Although this facility employed the same phenotyping platform (PlantArray; PlantDitech, Israel) and followed a similar measurement protocol, the experiments were conducted independently from those at the I-CORE centre in Rehovot. Data were collected using the SPAC analytics system and included plant biomass and transpiration measurements from experiments carried out between 17 April 2024 and 16 November 2024.

For external testing, we selected three individual plants, each from a different experiment. Since the Tel Aviv team includes soil bulk weight in their lysimeter measurements, we standardised the data sets by adjusting the initial seedling biomass to 10 g to match the conventions used in our own experiments, where only net plant biomass is recorded. This adjustment ensured consistency and comparability between the data sets.

The second external data set was collected from our indoor growth room (Room 101; Figure S2), located within the I-CORE centre, but operated under different environmental conditions and experimental constraints compared to the main greenhouse. This data set offers an independent context due to the

TABLE 2 | Hyperparameters. Adjusting these parameters change the learning ability, so the model would not underfit neither overfit the data set.

Model	Hyperparameter	Explanation	Options	Optimal value	Combinations
Decision Tree	min_samples_split	The minimum number of samples required to split an internal node.	[2, 3, 4]	4	60 candidates × five-folds = 300 fits
	min_samples_leaf	The minimum number of samples required to be at a leaf node of the trees.	[1, 2, 3, 4]	4	
	max_depth	The maximum depth of a decision tree.	[None, 5, 7, 10, 12]	10	
	n_estimators	The number of decision trees (estimators) or boosting rounds in the random forest ensemble.	[50, 60, 70, 80, 100]	100	240 candidates × five-folds = 1200 fits
	min_samples_split	Explained above	[2, 3, 4, 5]	4	
	min_samples_leaf	Explained above	[1, 2]	1	
	max_depth	Explained above	[None, 12, 15]	15	
XGBoost	bootstrap	This hyperparameter determines whether bootstrap samples (sampling with replacement) are used when building trees in the random forest.	[True, False]	True	
	n_estimators	Explained above	[60, 80, 100]	100	1296 candidates × 5 folds = 6480 fits
	min_child_weight	Minimum sum of sample weight (hessian) of the smallest leaf node. Larger values, preventing splits that have a smaller hessian value.	[1, 2, 4, 5]	1	
	max_depth	Explained above	[3, 5, 6, 7]	7	
	gamma	Minimum loss reduction required to make a further partition on a leaf node of the tree (helps in pruning the tree).	[0, 0.1, 0.2]	0	
Neural Network	reg_lambda	L2 regularisation term on weights. It adds a penalty to the loss function based on the size of the weights.	[0, 1, 2]	0	
	learning_rate	scales the contribution of each tree in the ensemble. A smaller learning rate makes the algorithm more robust by reducing the step size.	[0.3, 0.1, 0.01]	0.1	
	num_units – layer 1	controls the number of units (neurons) in each hidden layer of the neural network. It represents the width of the network.	[32, 64, 96, 128, 160, 192, 224, 256, 288]	32	1296 candidates × 40 epoch = 51 840 fits
	num_units – layer 2	Explained above	[32, 64, 96, 128, 160, 192, 224, 256, 288]	288	
	optimiser	determines the optimisation algorithm used to update the model's weights during training. The code considers	['adam', 'rmsprop']	rmsprop	

(Continues)

TABLE 2 | (Continued)

Model	Hyperparameter	Explanation	Options	Optimal value	Combinations
		two options: 'adam' (Adaptive Moment Estimation) and 'rmsprop' (Root Mean Square Propagation)			
	Activation - Layer1	The activation function applied to the output of each neuron in the hidden layers. Common choices are 'relu' (Rectified Linear Unit) and 'tanh' (Hyperbolic Tangent). Activation functions introduce non-linearity to the network, enabling it to learn complex patterns.	['relu', 'tanh']	tanh	
	Activation- Layer 2	Explained above	['relu', 'tanh']	tanh	
	learning_rate	The learning rate controls the step size at which the optimiser updates the model's weights in each iteration during training. It is a crucial hyperparameter as it affects the speed and stability of training.	[0.001, 0.01]	0.01	

Note: Implementing GridSearch cross-validation on 90% of the training data set. Systematically all the possible combinations of the hyperparameter options were evaluated, and the optimal setting was retained. We used the five-fold cross-validation splitting strategy to test the optimal parameters on five different subsets of the training data set.

controlled lighting, humidity and temperature conditions specific to growth room setups.

Both external data sets were evaluated using our Model Testing App, a web-based interface designed to assess model performance on new user-provided data sets. Users with SPAC analytics access can upload their experimental data and receive transpiration predictions generated by our pre-trained models, along with performance metrics for direct comparison against measured values. The application is publicly available at: <https://test-daily-transpiration-model-spac-user.streamlit.app/>.

2.11 | Feature Importance

To interpret the predictions and understand the importance and contribution of each feature to building the models several feature important tests were presented.

2.11.1 | Impurity-Based Feature Importance

Impurity-based feature importance is a technique commonly employed in decision tree-based machine learning models to assess the significance of individual features in making predictions. The method calculates the contribution of each feature by measuring how much it reduces the impurity (e.g., Gini impurity or entropy) in the model's decision nodes. This approach is simple, computationally efficient and interpretable, as it provides a clear ranking of features based on their impact. However, Impurity-based feature importance tends to favour variables with more categories or levels, which can lead to biases.

2.11.2 | Permutation Feature Importance

Permutation feature importance is a technique used to evaluate the significance of individual features in a machine learning model. The process involves systematically shuffling the values of a single feature in the data set and observing the impact on the model's performance. By comparing the model's performance before and after the permutation, a decrease in performance indicates that the feature is crucial, as its alteration disrupts the model's predictive accuracy. This approach does not require retraining the model and can be applied to various algorithms (not just tree-based models). However, it may not capture feature interactions and is most effective when dealing with uncorrelated features. In our study, the 'sklearn.inspection.permutation_importance' was used.

2.11.3 | SHAP

SHAP by Lundberg et al. (2017) is a method to explain individual predictions. SHAP is based on the game-theoretically optimal Shapley values (Molnar 2022). Shapley values provide a mathematically fair and unique method to attribute the payoff of a cooperative game to the players of the game (Merrick and Taly 2020; Shapley 1953). SHAP values help us understand the role of each feature in a prediction by calculating how much

each feature has pushed the prediction higher or lower, compared to the prediction without that feature. For instance, applying SHAP to our model (Figure S4 and see Figure 6) revealed that temperature significantly influences predicted daily transpiration. Lower temperatures (depicted in blue) correlate with negative SHAP values, pushing predictions downward, while higher temperatures (depicted in red) associate with positive SHAP values, pushing predictions upward. Therefore, in this context, the model suggests that transpiration tends to be lower at lower temperatures. The SHAP library in Python was used (Lundberg et al. 2017). For more info, see https://shap.readthedocs.io/en/latest/example_notebooks/api_examples/plots/beeswarm.html#.

2.11.4 | Ablation Analysis

In addition to the full feature set (Table 1), which included plant biomass as a predictor, we evaluated several ablation feature sets to test model robustness (Table 6). These included (i) a model excluding plant biomass, (ii) an age-based model in which 'plant age' (days since the start of recording) was used as a minimal proxy for plant size, (iii) a model excluding temperature and (iv) a minimal-predictors model restricted to temperature, plant biomass and soil type. It is important to note that plant age does not represent true biological age, as recording did not necessarily begin at the same developmental stage; all plants were assigned 'day 1' at the start of logging, regardless of initial size. All ablation models were trained and evaluated using the same preprocessing steps, hyperparameters and cross-validation strategy as described above, ensuring full comparability with the full models.

2.12 | Statistical Analysis

Several statistical methods were employed in this study. To assess the correlation between features, we used the correlation coefficient (r), which measures the strength and direction of the linear relationship between two variables. For evaluating model performance, we used R^2 (coefficient of determination), which represents the proportion of variance in the dependent variable that is predictable from the independent variables. t -tests were used to compare the means of two groups and to assess whether there were significant differences between them. p values associated with the t -tests were used to determine statistical significance, with a threshold of $p < 0.05$ considered significant.

For categorical variables, we used a chi-square test to evaluate associations between categories. The chi-square value indicates the magnitude of the discrepancy between observed and expected values, while the p value reveals whether this discrepancy is statistically significant. To compare multiple groups and determine whether their means differed significantly, we applied analysis of variance (ANOVA), calculating the F -statistic and corresponding p value to evaluate overall model significance. In addition, when group variances were unequal, we used Welch's test as a robust alternative to ANOVA, reporting the F -ratio and p value to verify the statistical significance of the differences.

3 | Results

From June 2018 to March 2024, multiple experiments were conducted in our greenhouses using the PlantArray systems. These experiments yielded continuous data on both plant physiology and environmental conditions. We collected, cleaned, labelled and averaged the data to obtain daily values, as described in the methods Section 2.4. For this study, we have used only well-irrigated data (soil water content at the end of the day was higher than the total daily transpiration; see Section 2.3.2), resulting in a data set comprising 6115 observations, with each observation representing a single plant, and its ambient conditions in a day of measurement.

This article investigates the environmental responses of tomato and cereal crops, cultivated during summer and winter seasons, respectively. Our findings reveal significant differences in environmental conditions between the two (Figure 4A and Figure S3). Tomato plants were exposed to significantly higher summer temperatures (grand mean 25.3°C for tomatoes and 18.6°C for cereals, $p < 0.001$; Figure 4A1) and RH (grand mean 56.15% for tomatoes and 52.49% for cereals, $p < 0.001$; Figure 4A2) compared to the winter conditions experienced by the cereals. Consequently, tomato plants were exposed to higher daily average VPD than cereals (grand mean 1.53 and 1.22 Kpa, respectively; $p < 0.001$; Figure 4A3). The DLI for tomatoes was also greater ($p < 0.001$), with an average of 18.27 mol/m²/day and a peak of 33.99 mol/m²/day, whereas cereals recorded a lower average DLI of 11.36 mol/m²/day and a maximum of 28.96 mol/m²/day (Figure 4A4).

Despite cereals having a higher average plant biomass (148.67 g) compared to tomatoes (111.54 g), their transpiration rates were significantly lower than those of tomatoes (average 160.24 and 318.32 g/day respectively; $p < 0.001$; Figures 4A5, 4A6). This comparative analysis underscores the distinct environmental adaptabilities and physiological responses of these crops under varying seasonal conditions.

The data present a relatively high correlation between DLI and temperature ($r = 0.75$) and a minor correlation between transpiration and plant biomass ($r = 0.61$; Figure 4B). VPD is relatively correlated to temperature ($r = 0.67$), RH ($r = -0.71$) and DLI ($r = 0.54$) but not to transpiration ($r = 0.21$; Figure 4B).

3.1 | Model Precision and Accuracy

Machine learning models were trained using the features: plant biomass, temperature, RH, VPD, DLI, plant type and soil type to predict daily transpiration (Table 1). Hyperparameters for all models were finely tuned using a Cross-Validation GridSearch on 90% of the training data set.

Our final models underwent rigorous evaluation through a 10-fold cross-validation process. This involved partitioning the data set into 10 subsets, with 90% allocated for training and the remaining 10% for testing, repeated across 10 iterations. Such meticulous methodology facilitated comprehensive assessment under diverse training scenarios. To ensure robust performance evaluation, we conducted statistical analyses, including RMSE

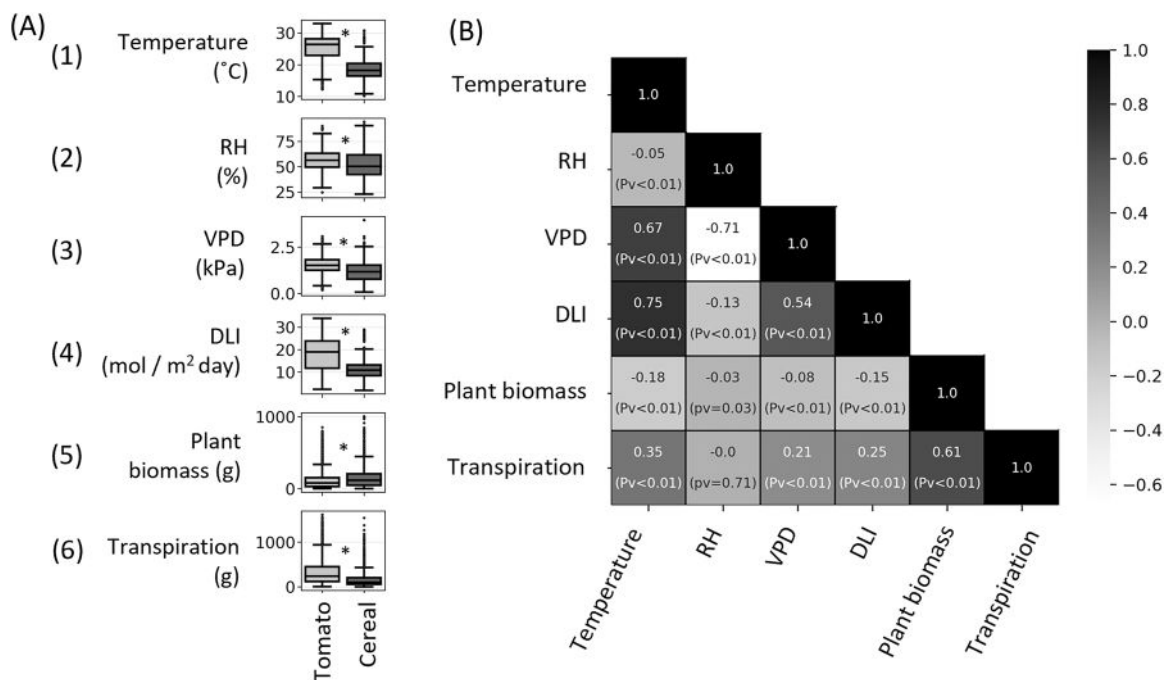


FIGURE 4 | Data visualisation. The data were collected between June 2018 and February 2022, by the lysimeter system, and preprocessed to daily values. (A) Data variety between tomato and cereal crops (3975/2140 observations respectively). Box and Whisker of daily (A1) temperature, (A2) RH, (A3) VPD, (A4) DLI, (A5) plant biomass and (A6) plant transpiration (for expansion see Figure S1). Asterisks indicate statistical difference, *t*-test; $p \leq 0.001$. (B) Pearson correlation coefficient chart of continuous features: Temperature, RH, VPD, DLI, plant biomass and transpiration (for expansion see Figure S1). *p* values are presented in brackets.

and R^2 calculations across the 10 folds. Notably, while the Decision Tree model displayed respectable performance, the models Random Forest, XGBoost and Neural Network showcased significant accuracy ($p < 0.05$, Table 3). Random Forest with the mean R^2 of 0.88 and an RMSE of 86.93. Similarly, XGBoost and Neural Network models yielded competitive mean R^2 values of 0.89 with RMSE values of 85.19 and 84.63, respectively. Neural Network, however, distinguished itself as the slowest model, completing the 10-fold cross-validation in 9.66 min ($p < 0.05$, Table 3).

3.2 | Testing the Models Using Holdout Experiments

Randomly selected experiments were separated from the rest of the data to serve as a validation data set for testing the models' performance on unseen data. The holdout data structure was different from the data used to tune and train the models; with a lower temperature (*t*-test = 14, $p \leq 0.001$), a different ratio of Tomato: Cereal (Chi-square = 94, $p < 0.001$), and a higher correlation between plant biomass and transpiration (Table S1, Figure S1). Moreover, the distribution of transpiration values in the holdout data significantly differed from those in the training data set ($p < 0.001$). Notably, the upper quartiles of transpiration in the training and holdout data sets were 379 and 255 g, respectively (Figures S5 and 5A). When the trained models were applied to this new data set, the Random Forest model demonstrated high accuracy in predicting transpiration, with a correlation coefficient (*r*) value of 0.91 (Figure 5B). The residual plot (Figure 5C) shows that the model's residuals are mostly centred around zero,

TABLE 3 | Comparison of evaluation scores among the four methods models.

Model	RMSE	R^2	Run time (sec)
Decision tree	104.51 ^a	0.83 ^a	0.01 ^a
Random forest	86.93 ^a	0.88 ^a	1.65 ^a
XGBoost	85.19 ^a	0.89 ^a	0.24 ^a
Neural Network	84.63 ^a	0.89 ^a	57.99 ^a

Note: The average of 10-fold cross-validations are presented. An ANOVA test was conducted to statistically evaluate performance differences among the 10-fold models scores, followed by Tukey's Honest Significant Difference (HSD), differences are indicated by letters.

^a $p < 0.05$.

indicating good predictive performance. Note that the distribution is wider where the transpiration is higher. The XGBoost exhibited the highest R^2 (0.82) and the lowest RMSE (88.41 g) among all models (Table 4, N.S.). The Random Forest Regressor model also performed well ($R^2 = 0.81$, RMSE = 90.77 g). Conversely, the Neural Network exhibited higher errors (N.S.), with an RMSE of 106 g and an MAE of 79.11 g. On the holdout data, Tukey HSD test revealed no significant differences between models (ANOVA: $F = 1.7$, $p = 0.15$).

Hyperparameter tuning (Table 2) slightly improved the XGBoost model performance on the holdout data, increasing R^2 from 0.807 to 0.81. To assess whether the tuning process improvement was statistically meaningful, we tested the tuning performance across 21 different random seeds, each resulting in a different holdout set. For each subset, we compared model performance

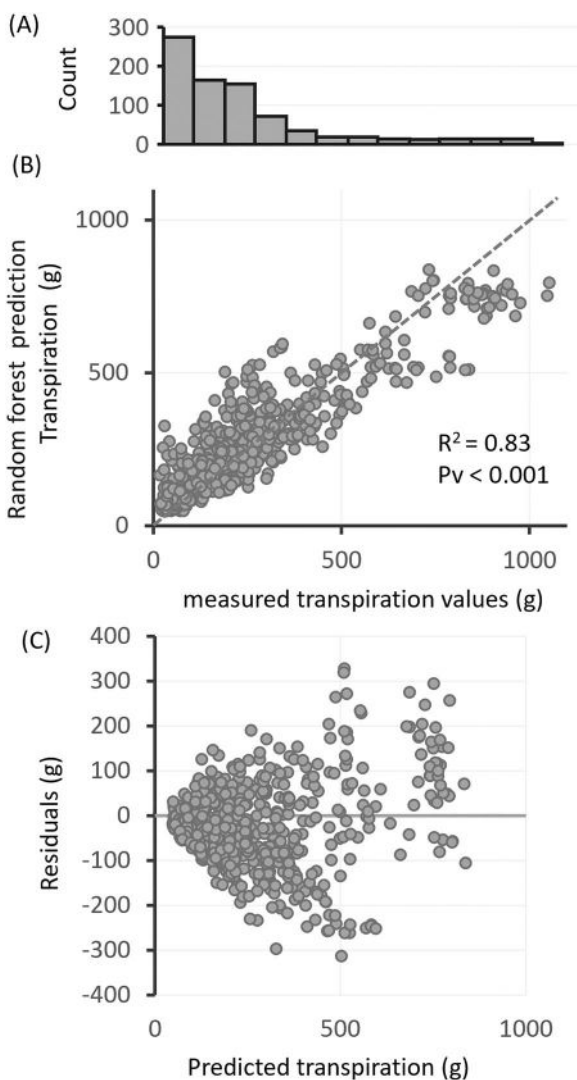


FIGURE 5 | Random forest model evaluation on five holdout experiments (A) Histogram distribution of daily transpiration measured in the holdout data. (B) Goodness of fit for the Random Forest model predictions, comparing predicted against observed values. The dashed grey line represents an exact fit ($Y = X$), indicating where the model's predictions perfectly match the observations. The R^2 and the associated p value are stated on the graph to indicate the strength and significance of the relationship. (C) Residuals (observed minus predicted values) plotted against predicted values to assess any systematic deviations from the model. Higher values, which are less frequent as shown in (A), exhibit increased scatter and reduced correlation, as illustrated in (B) and (C).

with and without hyperparameter tuning. There was no significant difference between the untuned and tuned models (RMSE difference of 0.19 g, paired t -test $p = 0.63$; Figure S6).

3.3 | Model Performance on Independent Greenhouse and Growth Room Experiments

To test the generalisability of our models, we evaluated them on two independent data sets: one from an externally operated greenhouse in Tel Aviv, and one from our controlled growth room (room 101). The Tel Aviv facility uses the same platform but is operated by a different team and follows independent

experimental procedures, while room 101 provides a distinct indoor environment managed by our own research group. For each experiment, a representative plant was selected to evaluate the models. For more details, see Section 2.10.

The models showed good performance on tomato plants across both sites. In Tel Aviv, the Random Forest model achieved an R^2 of 0.71, while in room 101 it reached 0.76, with lower RMSE in the latter. For cereal plants in Tel Aviv, XGBoost achieved the lowest RMSE (58.12 g), but the R^2 was only 0.33, indicating less consistency in capturing variability.

3.4 | Feature Importance

Feature importance was assessed through various techniques. For tree-based models, impurity metrics were employed, permutation and SHAP values were used. Interestingly, plant biomass and temperature were identified as crucial predictors for transpiration (Figure 6A) and the SHAP feature importance test (Figure 6B) on the Random Forest model predicting transpiration. The horizontal spread of dots for each feature indicates the range of SHAP values, with a wider spread denoting greater impact variability on model output. Colour signifies feature value magnitude, with red indicating high and blue indicating low values. Plant biomass, temperature and potting media are the most influential features in predicting transpiration, as evidenced by the wider spread of SHAP values, indicating a stronger effect on model predictions. In contrast, VPD and DLI show a narrow spread with randomly distributed colours, suggesting a small and uniform influence on model output. Divergent colour patterns in potting media reveal varying impacts on predictions, with soil (encoded as 1) increasing transpiration and sand (encoded as 0) decreasing it. Furthermore, the cereal plant type (encoded as 1) is associated with reduced transpiration, while the tomato (encoded as 0) contributes to increased transpiration.

To further evaluate the contribution of individual predictors, we conducted ablation analyses in which plant biomass or temperature was removed (Table 6). Excluding plant biomass, identified as the most important feature, caused the largest drop in performance, with holdout R^2 decreasing from 0.81 to 0.27 and RMSE increasing from 90.77 to 176.88 g. To test whether plant age could serve as a coarse proxy for size, we added this variable based on its correlation with plant biomass ($r = 0.7$, Figure S1A). However, because plant age was imprecisely recorded due to arbitrary initialisation in the database, it only partially recovered model accuracy ($R^2 = 0.49$, RMSE = 147.61 g). Excluding temperature had a more moderate impact ($R^2 = 0.79$, RMSE = 95.26 g). A minimal-predictors model using only plant biomass, temperature and soil type retained relatively high performance ($R^2 = 0.75$, RMSE = 103.44 g).

3.5 | Holdout Data Splitting Methods

In this section, we assess the robustness of our data analysis using three distinct partitioning strategies: temporal splits, greenhouse-based splits and random experiment-based splits. These methods help us evaluate how reliable is our data and

TABLE 4 | Model evaluation statistics on the holdout experiment data.

Model	R^2	RMSE (g)	MAE	Relative error ^a (%)	Residual ^b (g)	Residual ^b (%)	Tukey HSD ^c
Decision Tree	0.77	98.65	75.53	64.71	75.53	64.71	a
Random Forest	0.81	90.77	69.71	60.12	69.71	60.12	a
XGBoost	0.82	88.41	66.71	57.37	66.71	57.37	a
Neural Network	0.74	106.00	79.11	64.60	79.11	64.60	a

Note: Different letters indicate significant difference in Tukey HSD test $p < 0.05$. If all models share the same letter (e.g., “a”), this indicates that there were no significant differences among models.

^aRelative error, also known as the Relative RMSE, is a measure that quantifies the accuracy of predictions relative to the scale of the actual values. It is calculated as the RMSE divided by the mean of the actual values.

^bThe mean absolute residual was calculated.

^cTukey test on the residuals between the predicted and actual values.

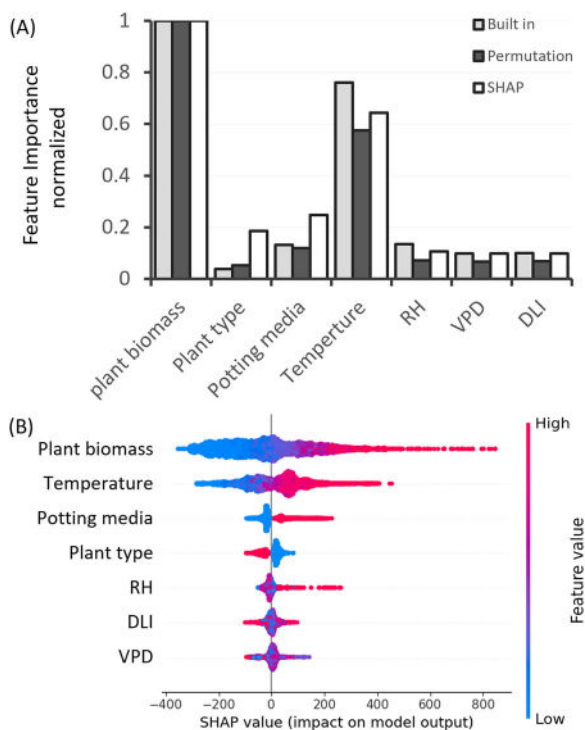


FIGURE 6 | Feature importance contribution to the model prediction accuracy. Plant biomass and temperature have a high importance overall. Testing feature significance in Random Forest model. (A) Feature importance using built-in impurity test (grey), permutation (black) and SHAP values (white). y-axes are the feature importance scores normalised by a Min-Max scaling method; a high score is given to the more influential features. (B) SHAP presentation of Feature importance. Every observation has one dot in each row. The position of the dot on the x-axis is the impact of that feature on the model's prediction for the observation, and the colour of the dot represents the value of that feature for the observation. A larger spread of dots suggests that the feature has a more significant impact on the model's predictions. [Color figure can be viewed at [wileyonlinelibrary.com](https://onlinelibrary.wiley.com)]

how well our models perform across different timeframes, environmental conditions and experimental setups.

For data partitioning, the temporal split involved segregating data by leaving out a different year for each iteration, using the remaining years for training. This approach allowed us to assess the model's ability to adapt to temporal variations. The

greenhouse-based split used data from one greenhouse for training and testing, while data from another was held out, enabling evaluation of model generalisability across different greenhouse environments. In the random experiment-based split, experiments were randomly selected as holdouts, with the remaining used for training, aiming to gauge the model's robustness across diverse experimental setups. R^2 scores analysis indicated no significant performance differences among the splitting methods: temporal split scored approximately 0.54 (median: 0.65), random experiment-based split achieved a mean of 0.62 (median: 0.60) and greenhouse-based split averaged 0.62 (Figure 7; Welch's test: $F = 0.68$, $p = 0.53$). Notably, variations in the random seed introduced considerable variability in the randomly selected holdout sets, while changes across different years also added diversity.

4 | Discussion

In this study, we explored the dynamics of daily transpiration in well-irrigated plants using advanced machine learning models. Our unique data set, collected over 7 years, included high-resolution physiological traits and meteorological measurements from two greenhouses. Our findings indicate that our ML models, particularly Random Forest and XGBoost, showed respectable performance in predicting daily transpiration. In addition, both SHAP and feature importance scores revealed that plant biomass and daily mean temperature are the most influential factors in these predictions. This discussion addresses these findings and their potential applications in agriculture.

4.1 | Seasonal Environmental Effects on Plant Biomass and Transpiration

Figure 4 highlights the distinct environmental parameters experienced by summer tomato and winter cereal, as well as the significantly higher daily transpiration of the tomatoes. Interestingly, the plant biomass (Figure 4A5) of cereals was significantly higher than that of tomatoes, with averages of 148.67 and 111.54 g, respectively. This result was unexpected, given the common correlation between larger annual plant size—which is closely related to transpiring leaf area (Halperin et al. 2017)—and higher transpiration rates (Figure 4B; Transpiration-Plant biomass; $r = 0.6$). However, this discrepancy highlights how seasonal environmental variations can influence transpiration.

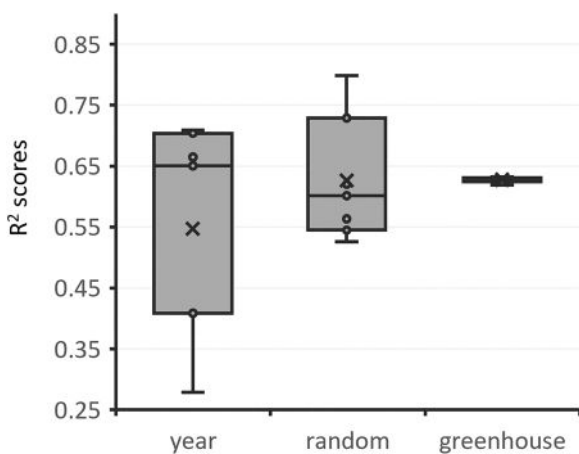


FIGURE 7 | Comparing data splitting methods for holdout data set. The distribution of R^2 scores for a tuned random forest model, evaluated using three distinct data splitting methods. The ‘Year’ method separates the data chronologically, training on observations from 6 years while holdout data were from one excluded year, repeatedly applied across all available years. The ‘Random’ method involves randomly selecting entire experiments as the holdout data set. Different random seeds lead to varied holdout experiments, resulting in a broad range of scores. The ‘Greenhouse’ method uses data from the main greenhouse for training and data from a secondary, different-sized greenhouse for testing.

4.2 | Model Performance and Accuracy

The effectiveness of ML models in predicting daily transpiration was tested. The tuned models were trained and evaluated using 10-fold cross-validation. Random Forest and XGBoost performed similarly, with XGBoost being seven times faster (Table 3). The XGBoost model achieved an RMSE of 85.19 g with an $R^2 = 0.89$. Neural Networks had comparable accuracy but much longer runtimes

Testing our model on a holdout data set, to further validate our model accuracy and generalisability. The XGBoost model demonstrates the strongest performance in predicting the daily transpiration ($R^2 = 0.82$, RMSE = 88.41 g), with no significant difference in the residuals between the XGBoost and the Random Forest models.

Interestingly, although hyperparameter tuning (Table 2) improved model performance slightly, testing tuning impact across different random seeds revealed that the improvement was not statistically significant on the holdout data (Figure S6). This lack of consistent performance gain may be due to the model already being well-calibrated with its default parameters, the limited benefit of tuning given the available feature set, or potential overfitting to the training data during the tuning process.

Our results align with other ML models that have predicted actual transpiration. For instance, Amir et al. (2021) reported that their Random Forest model had $R^2 = 0.81$, when predicting sap flow in cherry tomatoes. Similarly, Fan et al. (2021) achieved R^2 values from 0.816 to 0.95, using sap flow data from maize. Ohana-Levi et al. (2020) got R^2 values of up to 0.90 when predicting grapevine water consumption using drainage lysimeter data. Pagano et al. (2023) present a table summarising

several studies that predicted actual transpiration, with an average maximum R^2 of 0.87 for these predictions. We propose that the accuracy of our models ($R^2 = 0.81$ – 0.89) can be attributed to the precision of our transpiration measurements, the size of our data set, and the specific features used during model training (Table 1). Overall, these findings validate the possibility of using ML models to predict daily transpiration.

Testing our models on other experimental setups, demonstrate the models practical application and external validity in independent environments (Table 5). This external validation provides meaningful insights into the robustness, consistency and adaptability of our models under varying conditions. Notably, the optimal model differed depending on the plant type and environment. For tomato plants grown in both the Tel Aviv greenhouse and our controlled growth room (Room 101), the Random Forest model outperformed others, achieving R^2 values of 0.71 and 0.76, with corresponding RMSE values of 81.38 and 59.58 g, respectively. These results are consistent with the strong performance observed in our holdout experiments (see Figure 5), reinforcing the model’s reliability. In contrast, for cereal plants grown in Tel Aviv, the XGBoost model demonstrated the lowest RMSE (58.12 g), suggesting high predictive precision. However, the relatively low R^2 of 0.33 indicated that, while the model’s predictions were close in absolute terms (low RMSE), they did not align well with the variation in actual transpiration values—suggesting that the model failed to explain the full range of responses observed in the cereal plants. This may be due to the lower representation of cereal data (2140 observation vs. 3975 for tomato) and the narrower range of environmental condition under which cereal were grown, as evidence in Figure 4A (temperature and DLI) which show reduce variability for cereal compared to tomatoes. This divergence in model performance across plant types and conditions emphasises the importance of model selection tailored to specific experimental contexts.

We suggest that future work should expand the quantity and variability of our labelled data sets by periodically pooling standardised data from additional lysimeter installations. This would enhance model robustness and enable validation across a broader range of crops and climatic conditions. As this global data set matures, it may become necessary to develop a simple calibration factor—analogue to the FAO-56 crop coefficient—to harmonise measurements across different systems.

4.3 | Key Factors Influencing Transpiration

Artificial Intelligence models are often considered ‘black boxes’ due to their complexity, consideration of multiple parameters and the intricate statistical calculations involved in their algorithms (Azodi et al. 2020). Feature importance analysis enables us to understand the strength of each feature in the model’s predictions and in the transpiration processes.

Our Feature importance analysis indicates that **plant biomass** plays the most significant role in predicting daily transpiration (Figure 6). We find this result very rational as the correlation between plant biomass and transpiration is well known (Lambers et al. 2008; Lazar 2003). As larger plants have more leaves (and

thus more stomata) leading to more water loss. Similarly, other studies have found that canopy size in olives (Sperling et al. 2023) and plant height in maize (Z. Chen et al. 2020) are crucial factors. In addition, leaf area index has been effectively used in other studies to predict sap flow (Balasubramanian and Thirugnanam 2023), or grapevine water consumption (Ohana-Levi et al. 2020) highlighting the broader applicability of leaf and plant size in transpiration models.

We also tested whether plant age could serve as a proxy for plant biomass, as higher transpiration rates are often observed during late vegetative stages (Grulke and Retzlaff 2001; Juarez-Lopez et al. 2008). However, in our data, the correlation between plant age and transpiration is weak (days-transpiration; $r=0.38$, Figure S1), primarily due to inconsistencies in age recording: All plants were assigned ‘day 1’ at the start of logging, regardless of their true developmental stage. Nevertheless, including plant age in the ablation model partially recovered accuracy compared to the excluded-plant-biomass model (R^2 increasing from 0.27 to 0.49; RMSE decreasing from 176.88 to 147.61 g; Table 6), indicating that age does contain useful information despite its limitations.

Although direct measurement of plant biomass may not be practical in large-scale field applications, our findings suggest that accurately recorded plant age could serve as a practical alternative or complement. Future work could explore remote sensing or image-based methods as scalable alternatives to integrate plant size metrics into transpiration models.

VPD integrates the effects of both temperature and RH, with the literature often treating them as equally influential on transpiration. However, these two environmental factors not only interact reciprocally—such that a rise in temperature typically coincides with a decrease in RH, and vice versa—but also have distinct direct impacts on plant physiology. For example, while RH

primarily affects the atmospheric demand for water vapour, temperature directly influences enzymatic activity and metabolic processes within the plant. As a result, separating the independent contributions of temperature and RH to transpiration responses is challenging. Although VPD has traditionally been considered a key factor influencing stomatal conductance and overall plant transpiration (Song et al. 2022; Tanny 2013; Zhou et al. 2019), several studies have acknowledged the difficulty of disentangling these interdependent drivers (Bunce 2006; Grossiord et al. 2020), often focusing on VPD as the primary determinant of water loss rather than parsing the relative roles of its components. Against this backdrop, the findings from this study indicate that temperature exerts a greater influence than RH.

In fact, **temperature** was the second most important factor in our feature importance hierarchy, making it our most critical environmental predictor of daily transpiration (Figure 6). This aligns with its previously observed effects on physiological processes, as high temperatures drive transpiration by increasing water vapour pressure (Aschale et al. 2023; W. Liu et al. 2020). In addition, it directly affects the physiological responses of plants, such as stomatal conductance (Haijun et al. 2015). Some researchers even found temperature to be the most critical factor influencing evapotranspiration (ET₀), especially in spring and summer season when it contributes to as much as 46% of the variance of ET₀ (Aschale et al. 2023; W. Liu et al. 2020). Nevertheless, our results suggest that temperature alone may have a much stronger effect than RH. Thus, the high feature importance assigned to temperature in our model may indicate its predominant role in controlling transpiration, independent of the RH component of VPD. Notably, excluding temperature from the feature set had only a minor effect on model performance (Table 6), possibly because its influence is partially captured by the correlated VPD and RH variables. Further studies are needed to confirm and clarify this distinction.

TABLE 5 | Model performance on independent greenhouse experiments using the model testing app.

Greenhouse facility	Dates	Plant ID	Plant type	Best Model	RMSE (g)	R^2
Tel Aviv	15/07/2024–31/07/2024	2366	Tomato	Random forest	81.38	0.71
Tel Aviv	02/10/2024–16/11/2024	2470	Cereal	XGBoost	58.12	0.33
Room 101	13/09/2024–08/10/2024	638	Tomato	Random forest	59.58	0.76

TABLE 6 | Random forest model performance for daily transpiration prediction using alternative input sets.

Model Name	X variables	Test set		Holdout set	
		R^2	RMSE (g)	R^2	RMSE (g)
Baseline model	['VPD', 'Temp', 'RH', 'DLI', 'encoded_plant', 'encoded_soil', 'plant biomass']	0.88	86.93	0.81	90.77
Plant biomass excluded model	['VPD', 'Temp', 'RH', 'DLI', 'encoded_plant', 'encoded_soil']	0.78	119	0.27	176.88
Age-based model	['VPD', 'Temp', 'RH', 'DLI', 'days', 'encoded_plant', 'encoded_soil']	0.827	105.4	0.49	147.61
Temperature excluded model	['VPD', 'RH', 'DLI', 'encoded_plant', 'encoded_soil', 'plant biomass']	0.86	91.8	0.79	95.26
Minimal-predictors model	['Temp', 'plant biomass', 'encoded_soil']	0.809	111.02	0.75	103.44

Potting media is the third most important feature (Figure 6B). SHAP analysis showed that potting media are completely separated, and sand (blue) has negative effect on the transpiration compared to the soil (red). This is due to differences in water availability, as soil typically retains more water than sand, leading to higher transpiration in plants grown in soil (Cai et al. 2024).

We were surprised to find that **plant type** had a relatively low importance in predicting transpiration (Figure 6A). Genotype by Environment (GxE) interactions suggest that different crops like tomatoes and cereals, with potential variations in stomatal density, would influence transpiration rates (Des Marais et al. 2013; Fournier-Level et al. 2011). A possible explanation is that the model may identify plant type indirectly through biomass (Figure 4A5, Figure 6A). However, if the model's assessment holds, it could signal a ground-breaking insight into the plant transpiration prediction.

The low importance score of the **DLI** was unexpected, as it contradicts the common understanding of the high significance of solar radiation (Tanny 2013). It is possible that in indirect models based on eddy covariance (Pagano et al. 2023) and FAO56 estimation (Başagaoglu et al. 2021), radiation plays a more crucial role, whereas in models using direct measurements such as sap and lysimeters (current article), its importance may be less pronounced. Another consideration is that daily averaging might diminish the perceived importance of light, while more granular data collected at hourly or minute intervals may reveal its greater significance (as in these works: Kiraga et al. 2023; Li et al. 2020).

Future studies should explore the use of more granular data, such as hourly or minute-level measurements, instead of daily averages, to better capture the influence of all meteorological parameters on transpiration. Daily averaging can obscure the dynamic effects of factors like solar radiation, temperature and humidity, potentially underestimating their true importance. By analysing shorter time intervals, researchers may uncover stronger correlations between these variables and transpiration, providing a clearer understanding of their interactions.

It is important to note that soil water content, ambient CO₂ concentration and wind speed were maintained at non-stress or quasi-steady levels during the experiments (see Section 2) and were therefore not included as predictors. Because these variables are known to influence transpiration, future work should broaden the set of independent drivers and incorporate their dynamic behaviour into the machine-learning framework and model training.

We suggest that future elaboration and integration of additional ambient variables (such as CO₂ concentration, wind speed, soil electrical conductivity and soil water content) should be incorporated into the methodological framework proposed here. These factors exert direct, indirect and interactive effects on plant behaviour, and their inclusion could improve both the resolution of hierarchical environmental controls on whole-plant transpiration and the accuracy of transpiration prediction across a wider range of environmental conditions and growth systems.

4.4 | Splitting Methods

Splitting the data into train and validation sets can significantly impact model performance and generalisability (Shi et al. 2022). We explored three distinct data sampling methods: year (temporal), random and greenhouse (spatial). Although the models' accuracy results did not show a significant difference between them, each method offered unique insights into the data strengths and the models' ability to accurately predict transpiration (Figure 7). The year split had a median accuracy (R^2) of 0.65, impacted by greenhouse differences, equipment ageing and yearly meteorological variation. Random sampling yielded a median accuracy of 0.60, with a broader variation. Greenhouse-based splitting achieved 0.63, as the model effectively predicted transpiration in the secondary greenhouse using data from the main one, suggesting good generalisability across similar coupled setups.

4.5 | Future Applications and Model-Based Decision Support

In this study, we demonstrated that machine learning models can achieve respectable predictive performance using only a small number of input features. Moreover, the feature importance analysis reveals that the model's internal weighting aligns well with established physiological drivers of transpiration, reinforcing both its predictive value and biological relevance.

Future research should prioritise expanding the diversity, resolution and temporal coverage of environmental and physiological data by integrating advanced sensors for continuous spatiotemporal monitoring. This will enhance our ability to model dynamic plant-environment interactions with greater accuracy. In addition to improving prediction, AI models may enable early detection of suboptimal plant behaviour and stress responses, supporting proactive decision-making in precision agriculture. These future models are particularly valuable for disentangling multifactorial influences, such as the overlapping yet distinct effects of temperature and humidity, and for revealing non-intuitive interactions that might be overlooked in traditional analyses. Identifying the most influential variables also enables the strategic use of low-cost sensors in data-driven irrigation and environmental control systems. As data sets expand and model accuracy improves, predictions may increasingly rely on ambient measurements alone, with lysimeters serving primarily as initial calibration references. Ultimately, physiology-informed ML models can support scalable, sensor-efficient and predictive crop management, bridging fundamental understanding with real-world implementation.

Acknowledgements

This study was partly supported by the Shoenberg Research Center for Agricultural Science (Grant No. 3175006230), the Israel Science Foundation (Grant No. 1043/20) and the Israeli Committee for Budgeting, which support research on sustainable agriculture and food security at the Israeli Center for Digital Agriculture. This project was also funded by the Planning and Budgeting Committee of the Council for Higher Education in Israel (VATAT) as part of the programme 'Israeli Center for Digital Agriculture'. We are grateful to Dr. Nir Sade (Tel Aviv

University) for generously sharing data from his PlantArray phenotyping system. We also thank Prof. Assaf Mosquna, Prof. David Weiss, Prof. Dani Zamir and Prof. Zvi Peleg for kindly providing access to their data, which significantly contributed to this study.

Conflicts of Interest

The authors declare no conflicts of interest.

Data Availability Statement

Data available on request due to privacy/ethical restrictions.

References

- Abadi, M., A. Agarwal, P. Barham, et al. 2016. "TensorFlow: Large-Scale Machine Learning on Heterogeneous Distributed Systems." *ArXiv Preprint*, March 14. <https://doi.org/10.48550/arXiv.1603.04467>.
- Abyaneh, H. Z., A. M. Nia, M. B. Varkeshi, S. Marofi, and O. Kisi. 2011. "Performance Evaluation of ANN and ANFIS Models for Estimating Garlic Crop Evapotranspiration." *Journal of Irrigation and Drainage Engineering* 137, no. 5: 280–286. [https://doi.org/10.1061/\(ASCE\)IR.1943-4774.0000298](https://doi.org/10.1061/(ASCE)IR.1943-4774.0000298).
- Amani, S., and H. Shafizadeh-Moghadam. 2023. "A Review of Machine Learning Models and Influential Factors for Estimating Evapotranspiration Using Remote Sensing and Ground-Based Data." *Agricultural Water Management* 284: 108324. <https://doi.org/10.1016/J.AGWAT.2023.108324>.
- Amir, A., M. Butt, and O. Van Kooten. 2021. "Using Machine Learning Algorithms to Forecast the Sap Flow of Cherry Tomatoes in a Greenhouse." *IEEE Access* 9: 154183–154193. <https://doi.org/10.1109/ACCESS.2021.3127453>.
- Anapalli, S. S., L. R. Ahuja, P. H. Gowda, et al. 2016. "Simulation of Crop Evapotranspiration and Crop Coefficients With Data in Weighing Lysimeters." *Agricultural Water Management* 177: 274–283. <https://doi.org/10.1016/J.AGWAT.2016.08.009>.
- Anderegg, W. R. L., A. Wolf, A. Arango-Velez, et al. 2018. "Woody Plants Optimise Stomatal Behaviour Relative to Hydraulic Risk." *Ecology Letters* 21, no. 7: 968–977. <https://doi.org/10.1111/ELE.12962>.
- Aschale, T. M., D. J. Peres, A. Gullotta, G. Sciuto, and A. Cancelliere. 2023. "Trend Analysis and Identification of the Meteorological Factors Influencing Reference Evapotranspiration." *Water* 15, no. 3: 470. <https://doi.org/10.3390/W15030470>.
- Averbuch, N., and M. Moshelion. 2024. "Evaluating Evapotranspiration in a Commercial Greenhouse: A Comparative Study of Microclimatic Factors and Machine-Learning Algorithms." Preprint, *BioRxiv*, January 18. <https://doi.org/10.1101/2024.01.11.575151>.
- Azodi, C. B., J. Tang, and S. H. Shiu. 2020. "Opening the Black Box: Interpretable Machine Learning for Geneticists." *Trends in Genetics* 36, no. 6: 442–455. <https://doi.org/10.1016/J.TIG.2020.03.005/ASSET/2F2EDEAA-DCFE-4EB8-A287-6955F2A064F0/MAIN.ASSETS/GR3.JPG>.
- Balasubramanian, H. K., and H. Thirugnanam. 2023. "Neural Networking to Predict Sap Flow Using AI-Synthesized Relative Meteorological Data." 2023 3rd International Conference on Intelligent Technologies, CONIT 2023: 1–7. <https://doi.org/10.1109/CONIT59222.2023.10205886>.
- Ball, J. T., I. E. Woodrow, and J. A. Berry. 1987. "A Model Predicting Stomatal Conductance and Its Contribution to the Control of Photosynthesis Under Different Environmental Conditions." *Progress in Photosynthesis Research* 90, no. 1: 221–224. https://doi.org/10.1007/978-94-017-0519-6_48.
- Başağaoğlu, H., D. Chakraborty, and J. Winterle. 2021. "Reliable Evapotranspiration Predictions With a Probabilistic Machine Learning Framework." *Water* 2021 13, no. 4: 557. <https://doi.org/10.3390/W13040557>.
- Ben-Asher, J., A. Garcia Y Garcia, and G. Hoogenboom. 2008. "Effect of High Temperature on Photosynthesis and Transpiration of Sweet Corn (*Zea mays* L. Var. *rugosa*)." *Photosynthetica* 46, no. 4: 595–603. <https://doi.org/10.1007/S11099-008-0100-2>.
- Breiman, L. 2001. "Random Forests." *Machine Learning* 45, no. 1: 5–32. <https://doi.org/10.1023/A:1010933404324/METRICS>.
- Breiman, L., J. H. Friedman, R. A. Olshen, and C. J. Stone. 1984. *Classification and Regression Trees*. Routledge. 1st ed. <https://doi.org/10.1201/9781315139470>.
- Bunce, J. A. 2006. "How Do Leaf Hydraulics Limit Stomatal Conductance at High Water Vapour Pressure Deficits?" *Plant, Cell & Environment* 29, no. 8: 1644–1650. <https://doi.org/10.1111/J.1365-3040.2006.01541.X>.
- Cai, G., M. König, A. Carminati, et al. 2024. "Transpiration Response to Soil Drying and Vapor Pressure Deficit Is Soil Texture Specific." *Plant and Soil* 500, no. 1–2: 129–145. <https://doi.org/10.1007/s11104-022-05818-2>.
- Chen, T., and C. Guestrin. 2016. "XGBoost: A Scalable Tree Boosting System." In *Proceedings of the 22nd ACM SIGKDD International Conference on Knowledge Discovery and Data Mining*, 785–794. <https://doi.org/10.1145/2939672.2939785>.
- Chen, Z., S. Sun, Y. Wang, Q. Wang, and X. Zhang. 2020. "Temporal Convolution-Network-Based Models for Modeling Maize Evapotranspiration Under Mulched Drip Irrigation." *Computers and Electronics in Agriculture* 169: 105206. <https://doi.org/10.1016/J.COMPAG.2019.105206>.
- Chollet, F. 2015. "Keras: Deep Learning for Humans." <https://keras.io/>.
- Cutler, A., and G. Zhao. 2001. "PERT-Perfect Random Tree Ensembles." *Computing Science and Statistics* 33, no. 4: 90–94. <https://www.researchgate.net/publication/268424569>.
- Dalal, A., I. Shenhar, R. Bourstein, et al. 2020. "A Telemetric, Gravimetric Platform for Real-Time Physiological Phenotyping of Plant–Environment Interactions." *Journal of Visualized Experiments: JoVE* 162, no. e61280: 1–28. <https://doi.org/10.3791/61280>.
- Des Marais, D. L., K. M. Hernandez, and T. E. Juenger. 2013. "Genotype-by-Environment Interaction and Plasticity: Exploring Genomic Responses of Plants to the Abiotic Environment." *Annual Review of Ecology, Evolution, and Systematics* 44, no. 1: 5–29. <https://doi.org/10.1146/annurev-ecolsys-110512-135806>.
- Dixon, M., and J. Grace. 1984. "Effect of Wind on the Transpiration of Young Trees." *Annals of Botany* 53, no. 6: 811–819. <https://doi.org/10.1093/OXFORDJOURNALS.AOB.A086751>.
- Fan, J., J. Zheng, L. Wu, and F. Zhang. 2021. "Estimation of Daily Maize Transpiration Using Support Vector Machines, Extreme Gradient Boosting, Artificial and Deep Neural Networks Models." *Agricultural Water Management* 245: 106547. <https://doi.org/10.1016/J.AGWAT.2020.106547>.
- Ferreira, L. B., F. F. da Cunha, R. A. de Oliveira, and E. I. Fernandes Filho. 2019. "Estimation of Reference Evapotranspiration in Brazil With Limited Meteorological Data Using ANN and SVM—A New Approach." *Journal of Hydrology* 572: 556–570. <https://doi.org/10.1016/J.JHYDROL.2019.03.028>.
- Fournier-Level, A., A. Korte, M. D. Cooper, M. Nordborg, J. Schmitt, and A. M. Wilczek. 2011. "A Map of Local Adaptation in *Arabidopsis thaliana*." *Science* 334, no. 6052: 86–89. <https://doi.org/10.1126/science.1209271>.
- Fukushima, K. 1969. "Visual Feature Extraction by a Multilayered Network of Analog Threshold Elements." *IEEE Transactions on Systems Science and Cybernetics* 5, no. 4: 322–333. <https://doi.org/10.1109/TSSC.1969.300225>.
- Fürnkranz, J. 2011. "Decision Tree." In *Encyclopedia of Machine Learning*, 263–267. Springer. https://doi.org/10.1007/978-0-387-30164-8_204.
- Gaur, S., and D. T. Drewry. 2024. "Explainable Machine Learning for Predicting Stomatal Conductance Across Multiple Plant Functional Types." *Agricultural and Forest Meteorology* 350: 109955. <https://doi.org/10.1016/J.AGRFORMET.2024.109955>.
- Geller, G. N., and W. K. Smith. 1982. "Influence of Leaf Size, Orientation, and Arrangement on Temperature and Transpiration in Three

- High-Elevation, Large-Leafed Herbs." *Oecologia* 53, no. 2: 227–234. <https://doi.org/10.1007/BF00545668/METRICS>.
- Gosa, S. C., Y. Lupo, and M. Moshelion. 2019. "Quantitative and Comparative Analysis of Whole-Plant Performance for Functional Physiological Traits Phenotyping: New Tools to Support Pre-Breeding and Plant Stress Physiology Studies." *Plant Science* 282: 49–59. <https://doi.org/10.1016/J.PLANTSCI.2018.05.008>.
- Grossiord, C., T. N. Buckley, L. A. Cernusak, et al. 2020. "Plant Responses to Rising Vapor Pressure Deficit." *New Phytologist* 226, no. 6: 1550–1566. <https://doi.org/10.1111/NPH.16485;PAGE:STRING:ARTICLE/CHAPTER>.
- Grulke, N. E., and W. A. Retzlaff. 2001. "Changes in Physiological Attributes of Ponderosa Pine From Seedling to Mature Tree." *Tree Physiology* 21, no. 5: 275–286. <https://doi.org/10.1093/TREEPHYS/21.5.275>.
- Haijun, L., S. Cohen, J. H. Lemcoff, Y. Israeli, and J. Tanny. 2015. "Sap Flow, Canopy Conductance and Microclimate in a Banana Greenhouse." *Agricultural and Forest Meteorology* 201: 165–175. <https://doi.org/10.1016/j.agrformet.2014.11.009>.
- Halperin, O., A. Gebremedhin, R. Wallach, and M. Moshelion. 2017. "High-Throughput Physiological Phenotyping and Screening System for the Characterization of Plant–Environment Interactions." *Plant Journal* 89, no. 4: 839–850. <https://doi.org/10.1111/tj.13425>.
- Harris, C. R., K. J. Millman, S. J. van der Walt, et al. 2020. "Array Programming With NumPy." *Nature* 585, no. 7825: 357–362. <https://doi.org/10.1038/s41586-020-2649-2>.
- Haykin, S. 2009. *Neural Networks and Learning Machines*. Pearson Education India. 3rd ed.
- Ho, T. K. 1995. "Random Decision Forests." *Proceedings of the International Conference on Document Analysis and Recognition, ICDAR 1*: 278–282. <https://doi.org/10.1109/ICDAR.1995.598994>.
- Imai, K., and Y. Murata. 1976. "Effect of Carbon Dioxide Concentration on Growth and Dry Matter Production of Crop Plants: 1. Effects on Leaf Area, Dry Matter, Tillering, Dry Matter Distribution Ratio, and Transpiration." *Japanese Journal of Crop Science* 45, no. 4: 598–606.
- Iqbal, A., S. Fahad, M. Iqbal, et al. 2020. *Salt and Drought Stress Tolerance in Plants. Signaling and Communication in Plants*, edited by M. Hasanuzzaman, M. Tanveer, 77–118. Springer. https://doi.org/10.1007/978-3-030-40277-8_4.
- Juarez-Lopez, F. J., A. Escudero, and S. Mediavilla. 2008. "Ontogenetic Changes in Stomatal and Biochemical Limitations to Photosynthesis of Two Co-Occurring Mediterranean Oaks Differing in Leaf Life Span." *Tree Physiology* 28, no. 3: 367–374. <https://doi.org/10.1093/TREEPHYS/28.3.367>.
- Kiraga, S., R. T. Peters, B. Molaei, S. R. Evett, and G. Marek. 2023. "Reference Evapotranspiration Estimation Using Genetic Algorithm-Optimized Machine Learning Models and Standardized Penman-Monteith Equation in a Highly Arid Environment." *Water* 16, no. 1: 12. <https://doi.org/10.3390/w16010012>.
- Kumar, R., M. Hosseinzadehtaher, N. Hein, M. Shadmand, S. V. K. Jagadish, and B. Ghanbarian. 2022. "Challenges and Advances in Measuring Sap Flow in Agriculture and Agroforestry: A Review With Focus on Nuclear Magnetic Resonance." *Frontiers in Plant Science* 13: 1036078. <https://doi.org/10.3389/FPLS.2022.1036078/FULL>.
- Lambers, H., J. Raven, G. Shaver, and S. Smith. 2008. "Plant Nutrient-Acquisition Strategies Change With Soil Age." *Trends in Ecology & Evolution* 23, no. 2: 95–103. <https://doi.org/10.1016/J.TREE.2007.10.008/ASSET/CBF09F7C-765E-4123-ACAB-F9E82000E550/MAIN.ASSETS/GR3.JPG>.
- Landeras, G., A. Ortiz-Barredo, and J. J. López. 2008. "Comparison of Artificial Neural Network Models and Empirical and Semi-Empirical Equations for Daily Reference Evapotranspiration Estimation in the Basque Country (Northern Spain)." *Agricultural Water Management* 95, no. 5: 553–565. <https://doi.org/10.1016/J.AGWAT.2007.12.011>.
- Lange, O. L., R. Lössch, E. D. Schulze, and L. Kappen. 1971. "Responses of Stomata to Changes in Humidity." *Planta* 100, no. 1: 76–86. <https://doi.org/10.1007/BF00386887>.
- Lazar, T. 2003. "Taiz, L. and Zeiger, E. Plant Physiology. 3rd Edn." *Annals of Botany* 91, no. 6: 750–751. <https://doi.org/10.1093/AOB/MCG079>.
- von Leibniz, G. W. F. 1920. *The Early Mathematical Manuscripts of Leibniz*, edited by C. I. Gerhardt. Courier Corporation. <http://books.google.com/books?id=bOIGAAAAAAJ&oe=UTF-8>.
- Li, L., S. Chen, C. Yang, F. Meng, and N. Sigrimis. 2020. "Prediction of Plant Transpiration From Environmental Parameters and Relative Leaf Area Index Using the Random Forest Regression Algorithm." *Journal of Cleaner Production* 261: 121136. <https://doi.org/10.1016/J.JCLEPRO.2020.121136>.
- Lin, Y. S., B. E. Medlyn, R. A. Duursma, et al. 2015. "Optimal Stomatal Behaviour Around the World." *Nature Climate Change* 5, no. 5: 459–464. <https://doi.org/10.1038/NCLIMATE2550;SUBJMETA>.
- Liu, W., B. Zhang, and S. Han. 2020. "Quantitative Analysis of the Impact of Meteorological Factors on Reference Evapotranspiration Changes in Beijing, 1958–2017." *Water* 2020 12, no. 8: 2263. <https://doi.org/10.3390/W12082263>.
- Liu, X., C. Xu, X. Zhong, Y. Li, X. Yuan, and J. Cao. 2017. "Comparison of 16 Models for Reference Crop Evapotranspiration Against Weighing Lysimeter Measurement." *Agricultural Water Management* 184: 145–155. <https://doi.org/10.1016/J.AGWAT.2017.01.017>.
- López-Urrea, R., F. Martín de Santa Olalla, C. Fabeiro, and A. Moratalla. 2006. "Testing Evapotranspiration Equations Using Lysimeter Observations in a Semiarid Climate." *Agricultural Water Management* 85, no. 1–2: 15–26. <https://doi.org/10.1016/J.AGWAT.2006.03.014>.
- Lundberg, S. M., P. G. Allen, and S.-I. Lee. 2017. A Unified Approach to Interpreting Model Predictions. <https://github.com/slundberg/shap>.
- Madhu, M., and J. L. Hatfield. 2014. "Interaction of Carbon Dioxide Enrichment and Soil Moisture on Photosynthesis, Transpiration, and Water Use Efficiency of Soybean." *Agricultural Sciences* 05, no. 5: 410–429. <https://doi.org/10.4236/AS.2014.55043>.
- Mckinney, W. 2010. "Data Structures for Statistical Computing in Python." *Scipy* 445, no. 1: 51–56.
- Meneses, K. C., L. E. D. O. Aparecido, K. C. Meneses, and M. F. Farias. 2020. "Estimating Potential Evapotranspiration in Maranhão State Using Artificial Neural Networks." *Revista Brasileira de Meteorologia* 35, no. 4: 675–682. <https://doi.org/10.1590/0102-77863540072>.
- Merrick, L., and A. Taly. 2020. "The Explanation Game: Explaining Machine Learning Models Using Shapley Values." In *Machine Learning and Knowledge Extraction*, edited by A. Holzinger, Peter Kieseberg, a min Tjoa, and E. Weippl, 17–38. Springer International Publishing. https://doi.org/10.1007/978-3-030-57321-8_2.
- Mingers, J. 1989. "An Empirical Comparison of Selection Measures for Decision-Tree Induction." *Machine Learning* 1989 3, no. 4: 319–342. <https://doi.org/10.1007/BF00116837>.
- Molnar, C. 2022. *Chapter 9 Local Model-Agnostic Methods | Interpretable Machine Learning*. <https://christophm.github.io/interpretable-ml-book/local-methods.html>.
- Monteith, J. L. 1965. "Evaporation and Environment." *Symposia of the Society for Experimental Biology* 19: 205–234.
- Ohana-Levi, N., S. Munitz, A. Ben-Gal, A. Schwartz, A. Peeters, and Y. Netzer. 2020. "Multiseasonal Grapevine Water Consumption – Drivers and Forecasting." *Agricultural and Forest Meteorology* 280: 107796. <https://doi.org/10.1016/J.AGRFORMET.2019.107796>.
- Pagano, A., F. Amato, M. Ippolito, et al. 2023. "Machine Learning Models to Predict Daily Actual Evapotranspiration of Citrus Orchards Under Regulated Deficit Irrigation." *Ecological Informatics* 76: 102133. <https://doi.org/10.1016/J.ECOINF.2023.102133>.

- Pedregosa, F., V. Michel, O. Grisel, et al. 2011. "Scikit-Learn: Machine Learning in Python." *Journal of Machine Learning Research* 12, no. 85: 2825–2830. <http://jmlr.org/papers/v12/pedregosa11a.html>.
- Penman, H. L. 1948. "Natural Evaporation From Open Water, Hare Soil and Grass. Proceedings of the Royal Society of London." *Series A, Mathematical and Physical Sciences* 193, no. 1032: 120–145.
- Pieruschka, R., G. Huber, and J. A. Berry. 2010. "Control of Transpiration by Radiation." *Proceedings of the National Academy of Sciences* 107, no. 30: 13372–13377. <https://doi.org/10.1073/pnas.0913177107>.
- Quinlan, J. R. 1993. *C4.5: Programs for Machine Learning—J. Ross Quinlan - Google Books*. Morgan Kaufmann Publishers. [https://books.google.co.il/books?hl=en&lr=&id=b3ujBQAAQBAJ&oi=fnd&pg=PP1&dq=Quinlan,+J.+R.+\(1993\).%C2%A0C4.5:+Programs+for+machine+learning.+San+Mateo:+Morgan+Kaufmann.+&ots=ss1tRPJmC6&sig=d1hJNAHV650dcwNzQbol63WLRno&redir_esc=y#v=onepage&q=Quinlan%2C%20J.%20R.%20\(1993\).%C2%A0C4.5%3A%20Programs%20for%20machine%20learning.%20San%20Mateo%3A%20Morgan%20Kaufmann.&f=false](https://books.google.co.il/books?hl=en&lr=&id=b3ujBQAAQBAJ&oi=fnd&pg=PP1&dq=Quinlan,+J.+R.+(1993).%C2%A0C4.5:+Programs+for+machine+learning.+San+Mateo:+Morgan+Kaufmann.+&ots=ss1tRPJmC6&sig=d1hJNAHV650dcwNzQbol63WLRno&redir_esc=y#v=onepage&q=Quinlan%2C%20J.%20R.%20(1993).%C2%A0C4.5%3A%20Programs%20for%20machine%20learning.%20San%20Mateo%3A%20Morgan%20Kaufmann.&f=false).
- Rawson, H. M., J. E. Begg, and R. G. Woodward. 1977. "The Effect of Atmospheric Humidity on Photosynthesis, Transpiration and Water Use Efficiency of Leaves of Several Plant Species." *Planta* 134, no. 1: 5–10. <https://doi.org/10.1007/BF00390086/METRICS>.
- Rosenblatt, F. 1958. "The Perceptron: A Probabilistic Model for Information Storage and Organization in the Brain." *Psychological Review* 65, no. 6: 386–408. <https://doi.org/10.1037/H0042519>.
- Saunders, A., D. M. Drew, and W. Brink. 2021. "Machine Learning Models Perform Better Than Traditional Empirical Models for Stomatal Conductance When Applied to Multiple Tree Species Across Different Forest Biomes." *Trees, Forests and People* 6: 100139. <https://doi.org/10.1016/J.TFP.2021.100139>.
- Shapley, L. S. 1953. "17. A Value for n-Person Games." In *Contributions to the Theory of Games (AM-28)*, edited by H. W. Kuhn and A. W. Tucker, 2, 307–318. Princeton University Press. <https://doi.org/10.1515/9781400881970-018>.
- Shi, H., G. Luo, O. Hellwich, et al. 2022. "Evaluation of Water Flux Predictive Models Developed Using Eddy-Covariance Observations and Machine Learning: A Meta-Analysis." *Hydrology and Earth System Sciences* 26, no. 18: 4603–4618. <https://doi.org/10.5194/HESS-26-4603-2022>.
- Song, Y., W. Jiao, J. Wang, and L. Wang. 2022. "Increased Global Vegetation Productivity Despite Rising Atmospheric Dryness Over the Last Two Decades." *Earth's Future* 10, no. 7: e2021EF002634. <https://doi.org/10.1029/2021EF002634;WGROU:STRING:PUBLICATION>.
- Sperling, O., U. Yermiyahu, and U. Hochberg. 2023. "Linking Almond Trees' Transpiration to Irrigation's Mineral Composition by Physiological Indices and Machine Learning." *Irrigation Science* 41: 487–499. <https://doi.org/10.1007/s00271-022-00803-0>.
- Tanny, J. 2013. "Microclimate and Evapotranspiration of Crops Covered by Agricultural Screens: A Review." *Biosystems Engineering* 114, no. Issue 1: 26–43. <https://doi.org/10.1016/j.biosystemseng.2012.10.008>.
- The Pandas Development Team. 2020. *Pandas-Dev/Pandas: Pandas*. Zenodo. <https://doi.org/10.5281/ZENODO.10537285>.
- Virtanen, P., R. Gommers, T. E. Oliphant, et al. 2020. "SciPy 1.0: Fundamental Algorithms for Scientific Computing in Python." *Nature Methods* 17, no. 3: 261–272. <https://doi.org/10.1038/s41592-019-0686-2>.
- Xing, L., N. Cui, C. Liu, et al. 2022. "Estimation of Daily Apple Tree Transpiration in the Loess Plateau Region of China Using Deep Learning Models." *Agricultural Water Management* 273: 107889. <https://doi.org/10.1016/J.AGWAT.2022.107889>.
- Zhou, S., Y. Zhang, A. Park Williams, and P. Gentine. 2019. "Projected Increases in Intensity, Frequency, and Terrestrial Carbon Costs of Compound Drought and Aridity Events." *Science Advances* 5, no. 1: eaau5740. https://doi.org/10.1126/SCIADV.AAU5740/SUPPL_FILE/AAU5740_SM.PDF.

Supporting Information

Additional supporting information can be found online in the Supporting Information section.

Supplementary v4.